Università degli Studi di Napoli "Federico II"

PhD Program in

BIOLOGY

XXXVII Cycle

Macrophage engineering with genetic circuits to promote anti-tumor immune response

SUPERVISOR
Dr. Velia Siciliano

CANDIDATE
Ilaria De Martino

CO-SUPERVISOR
Prof. Caterina Missero

Ph.D. COORDINATOR
Prof. Sergio Esposito

Academic Year 2024-2025

Table of contents

Abstract

The tumor microenvironment (TME) is a complex and dynamic system that plays a pivotal role in cancer progression, immune evasion, and therapeutic resistance. Among the various components of the TME, tumor-associated macrophages (TAMs) are particularly influential due to their ability to transition between the pro-inflammatory, antitumorigenic M1 phenotype, and the immunosuppressive, pro-tumorigenic M2 phenotype. This plasticity makes TAMs key players in promoting tumor growth and dampening immune responses. The First, therapeutic strategies aimed at targeting TAMs have focused on their depletion from the TME, but these approaches often lack precision and fail to harness the full potential of macrophages in cancer therapy adequately. In contrast, synthetic biology offers the possibility to precisely control cellular behaviour, enabling the development of therapies that dynamically respond to the TME. During my PhD project, I investigated strategies to reprogram macrophages as microprocessor. Specifically, I developed potential therapeutic output (actuators) to programme macrophage function that can be coupled to sensing modules, which allow spatio-temporal control of their production. I focused on two actuators aiming at i) enhancing phagocytic activity of macrophages and ii) skewing macrophage polarization towards an M1 phenotype by expressing the **CV1 and Bacterial Compound (BC)** respectively. CV1 blocks the *don't eat me* axis based on the interaction of SIRPα-CD47. BC is a bacterial component that once bound to the toll-like receptor triggers a repolarization mechanism from M2 phenotype to M1 triggering an anti-inflammatory response. Our data suggest that this approach can help the reprogramming of TAMs, effectively converting them into potent antitumor agents while maintaining tight control over their activity. Importantly a sensing-actuating system like ours, while enhancing the immune responses, mitigates the challenges posed by the uncontrolled nature of traditional therapies. By reshaping the immunosuppressive TME, this strategy paves the way for the development of more advanced and effective cancer immunotherapies, underscoring the transformative potential of engineered macrophages in oncology.

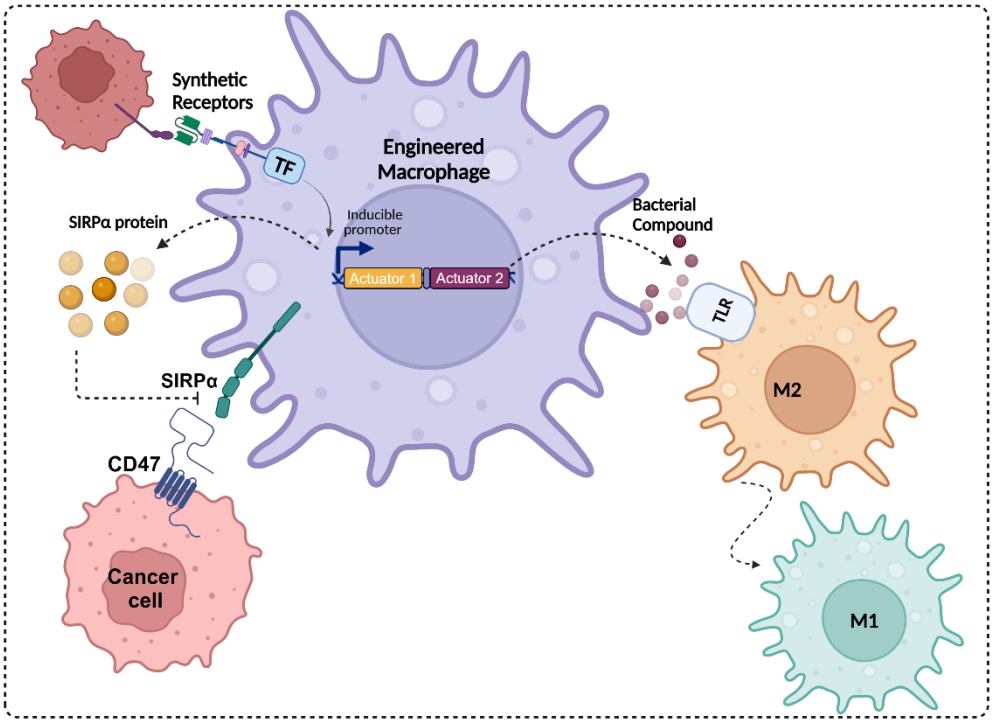

Figure 1 Synthetic biology approach to macrophage engineering. Development of a synthetic sensor-actuator system comprising a biosensor, based on a synthetic receptor sensitive to ligands in the tumor microenvironment (TME), and actuator models aiming at increasing phagocytosis and repolarizing macrophages from phenotype M2 to M1. The system designed in a way to be and activated when a specific ligand in the TME is bound by its specific synthetic receptor. The design of macrophages with synthetic actuators will allow local secretion of the SIRPα and Bacterial Compound (BC) proteins.

.

1 Introduction

1.1 Introduction to Synthetic Biology

The origins of synthetic biology can be traced back to the early 20th century with the advent of recombinant DNA technology[1]. However, it was not until the early 2000s that the term "synthetic biology" was coined, and the field began to take shape as a distinct discipline[2]. Key milestones include the development of the first synthetic genetic circuits, establishment of standardized biological parts (such as BioBricks[3],[4]), and the synthesis of the first fully synthetic genome in 2010 by the J. Craig Venter Institute[5]. Synthetic biology is an interdisciplinary field that merges principles from biology, engineering, chemistry, and computer science to design and construct new biological parts, devices, and systems or to redesign existing, natural biological systems for useful purposes[6]. This approach enables the creation of organisms with novel properties and functions that do not exist in nature, offering great potential for innovation and application across various industries. The field has traditionally focused on microbial systems, but recent advancements have extended to more complex eukaryotic systems, particularly mammalian cells[7]. Mammalian synthetic biology leverages these advancements to develop sophisticated biological tools and therapies that can address unmet medical needs.

1.1.1 Synthetic biology in therapeutics and cancer immunotherapy

Mammalian synthetic biology offers unparalleled opportunities to create innovative therapeutic strategies. By designing complex genetic circuits and integrating precise biological functions into mammalian cells, researchers can develop treatments that are highly specific, dynamic, and responsive to the pathological environment[8].

Synthetic biology techniques strive to achieve precise control over cellular functions by meticulously adjusting gene expression and therapeutic actions in reaction to specific biomarkers. This approach enables the development of 'programmable' systems designed to provide safer and more efficient treatments[9]. For therapeutic applications, sensing and actuating modules are integrated to form a responsive biological system that produces a desired outcome based on a specific input[10]. Various sensor modules can be employed to modify cellular behaviour in response to intracellular or extracellular signals. These signals are then processed and

translated into functional outputs through actuator modules that influence gene expression[11]. Several synthetic biology solutions have been developed for applications in therapeutics and cancer immunotherapy, highlighting its potential to revolutionize modern medicine. One of the most promising applications of mammalian synthetic biology is gene and cell therapy[6]. Engineered mammalian cells can deliver therapeutic genes to specific tissues, correct genetic defects, or produce therapeutic proteins in vivo[12].

- Gene and Cell Therapy

Engineered mammalian cells can deliver therapeutic genes to specific tissues, correct genetic defects, or produce therapeutic proteins in vivo. A prime example is CAR-T cell therapy, where T cells are engineered to express chimeric antigen receptors (CARs) that specifically target cancer cells. CAR-T cells have shown remarkable efficacy in treating haematological malignancies such as acute lymphoblastic leukaemia (ALL) and certain types of lymphomas[13] . This approach offers targeted killing of cancer cells while reducing off-target effects, significantly improving patient outcomes. Recent advances have also focused on engineering other immune cells, such as natural killer (NK) cells and macrophages, to improve their therapeutic potential[14].

- Smart Drug Delivery Systems

Synthetic biology also enables the creation of sophisticated drug-delivery systems that release therapeutic agents in response to specific molecular signals. These delivery systems enhance the precision and efficacy of treatments while minimizing side effects. For example, synthetic circuits can be engineered to release drugs in response to disease biomarkers, ensuring that the therapy is only active in the presence of the pathological condition. This is particularly beneficial for treating chronic diseases and conditions requiring long-term medication, as it reduces the frequency of administration and associated systemic side effects.[15]

- Regenerative Medicine

One application of mammalian synthetic biology in regenerative medicine, involves engineering stem cells with synthetic circuits to control their differentiation and proliferation. This allows for the development of advanced regenerative therapies that can replace damaged tissues and organs. Synthetic biology techniques have shown promise in treating a wide range of conditions, from neurodegenerative

diseases such as Parkinson's and Alzheimer's to tissue injuries like myocardial infarction and spinal cord injury. By precisely controlling stem cell behaviour, researchers can enhance tissue regeneration and repair, offering hope for previously untreatable conditions.[16]

- Tumor Microenvironment Challenges

The tumor microenvironment often presents barriers to an effective immune response, such as immunosuppressive cells and molecules that inhibit immune activity. Synthetic biology can create engineered cells capable of adapting to and modifying the tumor microenvironment, making it more conducive to immune cell activity and reducing resistance to therapy. This approach not only improves the targeting of cancer cells but also helps sustain the immune response over a longer period, reducing the chances of tumour relapse[17].

1.2 Tumor Microenvironment

The tumor microenvironment (TME) plays a pivotal role in cancer progression, metastasis, and response to therapies. Comprised of a dynamic and complex network of cells, signalling molecules, and extracellular matrix components, the TME significantly influences tumor behavior[18]. A crucial aspect of TME that garnered wide research interest was its first classification into "hot" and "cold" tumors[19]. This distinction is primarily based on the presence and activity of immune cells within the tumor microenvironment, which has profound implications for immunotherapy efficacy[20].

1.2.1 Cold and Hot Tumor

Hot tumors, also known as immunologically inflamed tumors, are characterized by a high infiltration of immune cells, particularly T cells. These tumors exhibit high levels of tumor-infiltrating lymphocytes (TILs), which are immune cells capable of recognizing and attacking cancer cells[21]. The presence of TILs, especially CD8+ cytotoxic T cells, is a hallmark of hot tumors and indicates an ongoing immune response against the tumor. Hot tumors also express immune checkpoint molecules, such as PD-L1 (Programmed Death-Ligand 1), which can interact with PD-1 on T cells to inhibit their activity. This mechanism allows tumors to evade immune surveillance by suppressing the function of T cells. Additionally, hot tumors often

have elevated levels of pro-inflammatory cytokines like IFN-γ (Interferon-gamma) and IL-2 (Interleukin-2), which further promote immune cell activation and recruitment. Hot tumors tend to respond well to immunotherapies, such as immune checkpoint inhibitors (e.g., anti-PD-1/PD-L1 and anti-CTLA-4). These treatments can reactivate T cells and enhance their ability to attack cancer cells. The pre-existing immune response in hot tumors provides a foundation for these immunotherapeutic strategies, making them more effective in patients with hot tumors[22,23].

In contrast, **Cold Tumors** are immunologically non-inflamed or excluded tumors. These tumors are characterized by a low infiltration of immune cells, indicating a lack of robust immune activity within the tumor microenvironment[24]. Cold tumors may employ various mechanisms to create an immunosuppressive environment, such as recruiting regulatory T cells (Tregs) and myeloid-derived suppressor cells (MDSCs), which inhibit effective anti-tumor immune responses[25]. Furthermore, cold tumors often exhibit defects in antigen presentation, such as downregulation of MHC class I molecules, making it difficult for immune cells to recognize and target cancer cells. The absence of pro-inflammatory cytokines and chemokines in cold tumors also contributes to the lack of immune cell infiltration and activation[26].

Given the significant impact of the TME on cancer progression and treatment response, several therapeutic strategies aim to modify the TME to enhance anti-tumor immunity. Immune checkpoint inhibitors work by blocking inhibitory pathways such as PD-1/PD-L1 and CTLA-4, reinvigorating exhausted T cells and promoting an anti-tumor response[27]. Oncolytic viruses can transform cold tumors into hot tumors by inducing an inflammatory response. Cancer vaccines targeting tumor-specific antigens aim to stimulate a targeted immune response, potentially altering the immune landscape of cold tumors. Adoptive cell transfer (ACT) involves the infusion of autologous or allogeneic T cells engineered to target tumor antigens, thereby enhancing the immune attack on tumors[20]. Combining immune checkpoint inhibitors with other therapies, such as radiation, chemotherapy, or targeted therapies, can synergistically modulate the TME and improve therapeutic outcomes[28].

1.3 Tumor-Associated Macrophages (TAMs)

As part of the innate immune system, macrophages are one of the first lines of defence in our organism, but they are also crucial for setting the adaptive immune response. Based on their origin, macrophages can be divided into two categories: tissue-resident macrophages and blood-recruited macrophages[29]. Tissue-resident macrophages derive from precursors of the yolk sac and fetal liver and acquire specialized functions that are specific to the tissue where they develop: Microglia (SNC); Kupfer cells (liver); Alveolar macrophages (lung); Osteoclasts (bone)[30] Alternatively, circulating monocytes, in case of local inflammation, can go out of the bloodstream into tissue and become macrophages[31]. In general, they play a key role in phagocytosis, cytokine release, antigen presentation, and antibody-mediated cell cytotoxicity (ADCC) and they are responsible for both tissue repair and protection from pathogens. Blood-derived macrophages are highly abundant within the tumor microenvironment (TME), as circulating monocytes are recruited to the tumor site by various chemotactic factors produced by cancer cells and stromal cells, such as CCL2, CCL5, and colony-stimulating factor 1 (CSF-1)[32]. Once within the TME, these monocytes differentiate into macrophages called tumor-associated macrophages (TAMs) under the influence of local signals including interleukin-10 (IL-10), transforming growth factor-beta (TGF-β), and hypoxia-induced factors. These macrophages possess distinct phenotypic functions that actively shape the TME[33]. One crucial aspect of TAMs' behavior is their ability to remodel the extracellular matrix (ECM). TAMs produce various proteolytic enzymes such as matrix metalloproteinases (MMPs), which promote ECM degradation and facilitate tumor invasion[34,35]. Moreover, TAMs establish reciprocal paracrine and cell-cell interactions with cancer stem cells (CSCs), a small subpopulation of cells within tumors with self-renewal and tumor-initiating capabilities. Through these interactions, TAMs provide crucial signalling cues and growth factors that support CSC maintenance and promote tumor growth[36]. Additionally, TAMs contribute to immune evasion by suppressing anti-tumor immune responses and promoting an immunosuppressive environment within the TME. The dual role of TAMs in supporting tumor growth and suppressing anti-tumor immune responses makes them a critical target for cancer therapies.[37,38]

1.3.1 Macrophages polarization

Depending on the stimuli received from the microenvironment, macrophages can adopt a large variety of phenotypes that allow us to classify them in M1 (pro-inflammatory) and M2 (anti-inflammatory). In 2000, Mills and colleagues attempted to categorize macrophage polarization states [39] . The polarization of TAMs into these phenotypes is influenced by various signals within the TME, including cytokines, growth factors, and hypoxic conditions, which collectively shape their behaviour and impact on tumor progression. Each polarized macrophage displays a differential expression profile of cytokines, enzymes, and cell-surface markers.M1 also known as classically activated macrophages, are induced by signals such as interferon-gamma (IFN-γ) and bacterial lipopolysaccharides (LPS)[40]. These macrophages are characterized by their production of pro-inflammatory cytokines like tumor necrosis factor-alpha (TNF-α), interleukin-6 (IL-6), and interleukin-12 (IL-12), as well as reactive oxygen species (ROS) and reactive nitrogen species (RNS). M1 plays a crucial role in mounting anti-tumor responses by enhancing the cytotoxic activity of T cells and natural killer (NK) cells, and by directly attacking tumor cells through the production of ROS and RNS[41]. Their presence in the TME is often associated with a robust anti-tumor immune response and tumor growth inhibition. Conversely, M2 or alternatively activated macrophages, arise in response to anti-inflammatory signals such as interleukin-4 (IL-4), interleukin-10 (IL-10), and interleukin-13 (IL-13) [42]. These macrophages are typically involved in tissue repair and immune regulation, characterized by the secretion of anti-inflammatory cytokines like IL-10 and transforming growth factor-beta (TGF-β), and the promotion of extracellular matrix remodelling and angiogenesis[43]. In the context of the TME, M2 supports tumor progression by creating an immunosuppressive environment that inhibits the activity of cytotoxic T cells and other anti-tumor immune cells. They also promote tumor growth and metastasis through the secretion of pro-angiogenic factors such as vascular endothelial growth factor (VEGF) and by facilitating the epithelial-mesenchymal transition (EMT) of cancer cells, which enhances their invasive potential[44]. The balance between M1 and M2 within the TME is dynamic and can significantly influence the course of tumor progression[45]. While M1 exerts anti-tumor effects, the predominant presence of M2 typically supports tumor growth and immune evasion. Understanding the mechanisms that govern TAMs polarization is

critical for developing therapeutic strategies aimed at reprogramming [46] TAMs to an M1 phenotype or inhibiting the pro-tumorigenic functions of M2 [47]. TAMs play a dual role in the TME, with their M1 and M2 phenotypes representing two ends of a spectrum of functional states that can either inhibit or promote tumor progression[48]. Targeting the plasticity and polarization of TAMs holds significant promise for novel cancer therapeutic approaches for reprogramming the TME to support anti-tumor immunity[49].

1.4 Macrophages in Cancer Immunotherapy

Cancer immunotherapies targeting adaptive immune checkpoints have substantially improved patient outcomes across multiple metastatic and treatment-refractory cancer types. However, emerging studies have demonstrated that innate immune checkpoints, which interfere with detecting and clearing malignant cells through phagocytosis and suppress innate immune sensing, also play a key role in tumor-mediated immune escape. Current strategies aiming to target macrophages for effective tumor immunotherapy include: i) inhibiting macrophage recruitment[50], ii) reducing macrophage survival[51,52], iii) modifying effector cells[51], iv) inducing phenotypic polarization[53], and v) inhibiting tumor-promoting functions[54–57]. Further understanding and manipulating these pathways, particularly through the "Don't Eat Me" signals and the repolarization of TAMs from a pro-tumorigenic to an anti-tumorigenic phenotype via Toll-like Receptor (TLR) activation, represents a promising avenue to enhance macrophage-mediated tumor clearance and overcome the immunosuppressive environment within the TME.

1.4.1 Mechanism of "Don't Eat Me" Signaling in Cancer Cells

Cancer cells employ various strategies to evade immune surveillance, including the "don't eat me" signal. This mechanism involves the expression of specific ligands on cancer cells that interact with macrophage receptors to inhibit their phagocytic activity. By activating these signals, the cancer cells effectively evade their recognition and destruction by the immune system. The best known of these binders is CD47 which recognizes the SIRPα receptor; however, recently other axes involved in this mechanism have been discovered MHC-I/LILRB1-CD24/SIGLEC10 and PD1/PDL1 (**Fig.2**).

- **Signal Regulatory Protein Alpha (SIRPα) and CD47 Interaction**

Identified in the late 1990s, the first member in the SIRP family, SIRPα, is a 115–120 kDa glycoprotein expressed on myeloid cells, including all types of macrophages[58,59]. SIRPα has an extracellular immunoglobulin domain, for ligand binding, that contains an N-terminal IgV domain followed by two IgC domains and a cytosolic domain that includes an immunoreceptor tyrosine-based inhibitory motif (ITIM), which enables its association with either SH2-containing protein tyrosine phosphatase 1 (SHP1; also known as PTPN6) or SHP2 (also known as PTPN11) for signal transduction[58,60] .

CD47 also known as integrin-associated protein (IAP), was first established as a membrane protein expressed on normal red blood cells (RBCs). CD47 has a long N-terminal extracellular domain and five transmembrane domains, as well as a short cytosolic domain[61].The extracellular IgV- like domain of CD47 is responsible for its interaction with the N- terminal IgV-like domain of SIRPα[47,48]. This CD47–SIRPα interaction results in the phosphorylation of two tyrosine residues in the intracellular ITIM of SIRPα[62,63]. These phosphorylated tyrosines on SIRPα recruit and activate SHP1 and SHP2, two phosphatases that dephosphorylate signaling intermediates involved in the reorganization of the actin cytoskeleton (Myosin IIA), ultimately leading to the inhibition of phagocytosis. This process halts the "engulfment" mechanism that would normally allow the macrophage to consume the target cells[64]. In healthy tissues, the CD47-SIRPα interaction is essential for distinguishing self-cells from non-self entities, preventing the immune system from attacking the body's own cells. However, cancer cells exploit this axis by overexpressing CD47 on their surface, thereby mimicking healthy cells and avoiding destruction by the immune system. This phenomenon has been documented in a wide range of cancers, including acute myeloid leukaemia, non-Hodgkin lymphoma, and solid tumors such as breast, ovarian, and lung cancers[65–67].

- **Sialic acid-binding Ig-like lectin 10 (SIGLEC-10) and CD24 interaction**

The CD24-Siglec-10 axis represents a newer mechanism by which cancer cells evade macrophage recognition, particularly through sialylated glycan interactions[68]. CD24 is highly expressed in various tumor cells and plays a crucial role in tumor development, invasion, and migration. It is recognized as a strong and independent molecular marker for the prognosis of ovarian cancer, while also being implicated in the growth and metastasis of breast cancer and potentially pancreatic cancer[69–72]. Notably, CD24 is most upregulated in triple-negative breast cancer (TNBC) and ovarian cancer, where it is associated with decreased recurrence-free survival (RFS) and overall survival (OS), respectively. CD24 acts as a "don't eat me" signal by interacting with the inhibitory receptor SIGLEC-10 on macrophages within the tumor microenvironment (TME), thereby functioning as an immune checkpoint[73]. Also known as heat-stable antigen or small-cell lung carcinoma cluster 4 antigen, CD24 is a heavily glycosylated glycosylphosphatidylinositol (GPI)-anchored surface protein[74]. It interacts with Siglec-10 on innate immune cells to suppress inflammatory responses in conditions such as infection, sepsis, liver damage, and chronic graft-versus-host disease. The sialic acid-binding immunoglobulin-like lectins (Siglecs) are type I transmembrane proteins characterized by varying numbers of immunoglobulin (Ig)-like domains, including C2-set domains and IgV-like domains, which are responsible for recognizing the N-terminal of ligands. Siglecs possess immune receptor tyrosine-based inhibitory motifs (ITIMs) or ITIM-like motifs, which play a crucial role in immune regulation by interacting with proteins containing SH2 domains, such as SHP-1 and SHP-2[75,74]. The binding of CD24 to Siglec-10 initiates an inhibitory signalling cascade. Upon ligand binding, Siglec-10’s ITIM motifs become phosphorylated, recruiting SHP-1 and SHP-2 phosphatases, which subsequently inhibit pro-phagocytic signalling pathway[74] This glycan-mediated interaction allows tumor cells to evade destruction by macrophages, fostering an immunosuppressive microenvironment.

- **LILRB1 and Major histocompatibility complex class I (MHC-I) interaction.**

The LILRB1-HLA-G pathway represents another critical immune escape mechanism. Leukocyte Immunoglobulin-Like Receptor B1 (LILRB1) is an inhibitory receptor expressed on various immune cells, including macrophages, dendritic cells, and NK cells[76]. Its ligand, HLA-G, is a non-classical MHC Class I molecule that plays a pivotal role in immune tolerance and inhibiting macrophage-mediated phagocytosis[77]. This complex, composed of HLA α-chains and β2-microglobulin (β2M), is often overexpressed in certain cancers as lung**,** breast**,** melanoma**,** and colorectal cancer to evade immune clearance[78,79] . Two receptors from the leukocyte immunoglobulin-like receptor (LILR) family, LILRB1 and LILRB2 have been identified, which interact with MHC-I but only LILRB1 was found to suppress phagocytosis. LILRB1—also known as CD85J, ILT2, or LIR-1—is widely expressed on myeloid and certain lymphoid cells, including macrophages, monocytes, dendritic cells (DCs), and T and B cell subsets[80,81]. Structurally, LILRB1 has four extracellular domains of IgC and a cytoplasmic tail containing ITIMs[82]. When LILRB1 makes contact with the β2M subunit of the MHCI complex, the ITIMs domains are phosphorylated and bind to SHP-1 thus inhibiting intracellular signalling and reducing phagocytic activity[77]. The MHC-I–LILRB1 axis plays a dual role in both adaptive and innate immune evasion. While MHC-I typically functions to present antigens to T cells, its interaction with LILRB1 on macrophages inhibits phagocytosis, allowing tumor cells to survive within the tumor microenvironment[77]. In cancer, especially in tumor-associated macrophages (TAMs), LILRB1 expression is elevated, further enhancing this immune escape mechanism. The β2M subunit is critical in mediating the species-specific interaction between MHC-I and LILRB1, making it an important target for therapeutic intervention aimed at reversing macrophage inhibition and promoting anti-tumor immunity.

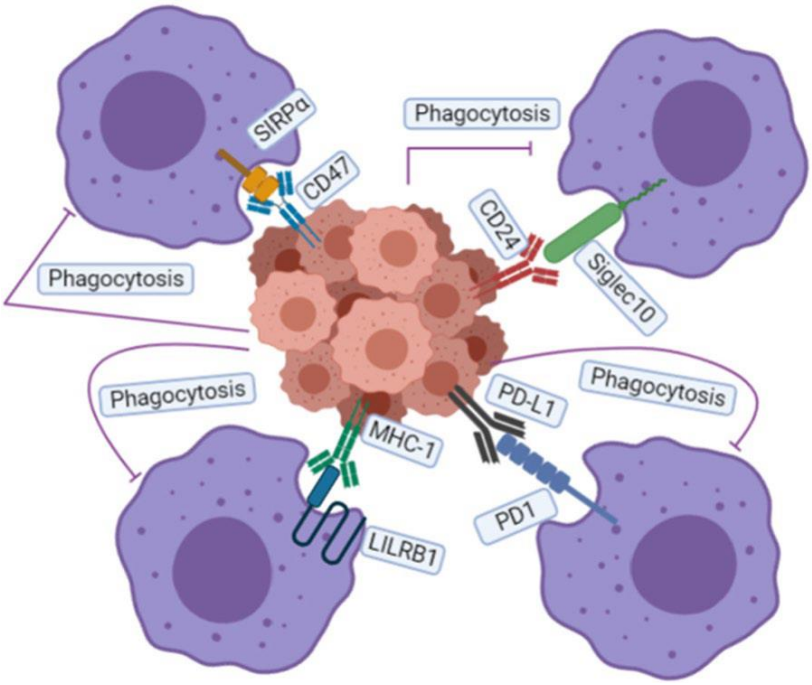

Figure 2 **Schematic representation of "Don't Eat Me Signal":** The CD47/SIRPα axis, PD-1/PD-L1 axis, MHC-I/LILRB1 axis, and CD24/SIGLEC-10 axis all play significant roles in inhibiting cancer cell engulfment, and disruption of these interactions can enhance the phagocytosis of macrophages. (From Wei Li, 2022)

1.4.2 Toll-Like Receptor and Its Role in Macrophage Re-Polarization

The ability to repolarize macrophages from an M2 to an M1 phenotype is of particular interest in cancer therapy, where tumor-associated macrophages (TAMs) often adopt an M2-like phenotype that promotes tumor growth and suppresses anti-tumor immunity. Toll-like receptors (TLRs) play a pivotal role in this macrophage plasticity, as their activation can drive the repolarization of M2 macrophages into M1, reawakening their tumoricidal functions by triggering the release of pro-mediators inflammatory and overstimulating antigen presentation[83].

Toll-like receptors (TLRs) are a family of pattern recognition receptors (PRRs) that play a critical role in detecting pathogen-associated molecular patterns (PAMPs) and damage-associated molecular patterns (DAMPs), initiating the innate immune response and bridging it with adaptive immunity[84]. The human genome encodes 10 TLRs (TLR1-TLR10), each specific to distinct ligands from pathogens, including bacteria, viruses, fungi, and parasites. Upon binding their respective ligands, TLRs activate intracellular signalling cascades that are largely mediated through two key adaptor proteins: myeloid differentiation primary-response gene 88 (MyD88) and Toll/IL-1 receptor-domain-containing adapter-inducing interferon-β (TRIF)[85]. These

pathways lead to the activation of transcription factors, such as nuclear factor kappa-β (NF-κβ) and activator protein-1 (AP-1), which promote the production of pro-inflammatory cytokines like TNF-α, IL-6, and IL-12, critical mediators of the M1 macrophage response[86,87]. TLRs are expressed on the cell surface or within endosomal compartments of immune cells such as macrophages, dendritic cells, neutrophils, and B cells, as well as non-immune cells like mucosal epithelial and endothelial cells. The strategic localization of TLRs in these distinct subcellular regions enables the detection of different pathogen-derived molecules, thereby eliciting the most appropriate immune response[88]. Upon ligand binding, TLRs undergo dimerization, triggering intracellular signalling through their Toll/interleukin-1 receptor (TIR) domains, resulting in the expression of inflammatory chemokines and cytokines. This inflammatory response recruits' additional immune cells, such as neutrophils and macrophages, to the site of infection or damage, amplifying the immune response[89]. TLR signalling is bifurcated into two primary pathways: the MyD88-dependent and TRIF-dependent pathways. MyD88, the most commonly utilized adaptor, facilitates signalling for all TLRs except TLR3. This pathway activates interleukin-1 receptor-associated kinase-1 (IRAK1), IRAK4, and TNF receptor-associated factor-6 (TRAF6), leading to the activation of NF-κB and AP-1, which are pivotal in upregulating pro-inflammatory cytokines[90]. TLR3 and TLR4, however, engage the TRIF-dependent pathway, which can activate NF-κB and interferon regulatory factor 3 (IRF3), the latter being crucial for the production of type I interferons with antiviral properties. Uniquely, TLR4 can switch between the MyD88-dependent pathway at the plasma membrane and the TRIF-dependent pathway when internalized into endosomes, where it requires a TRIF-related adaptor molecule (TRAM) for full activation[91] (**Fig.3**).

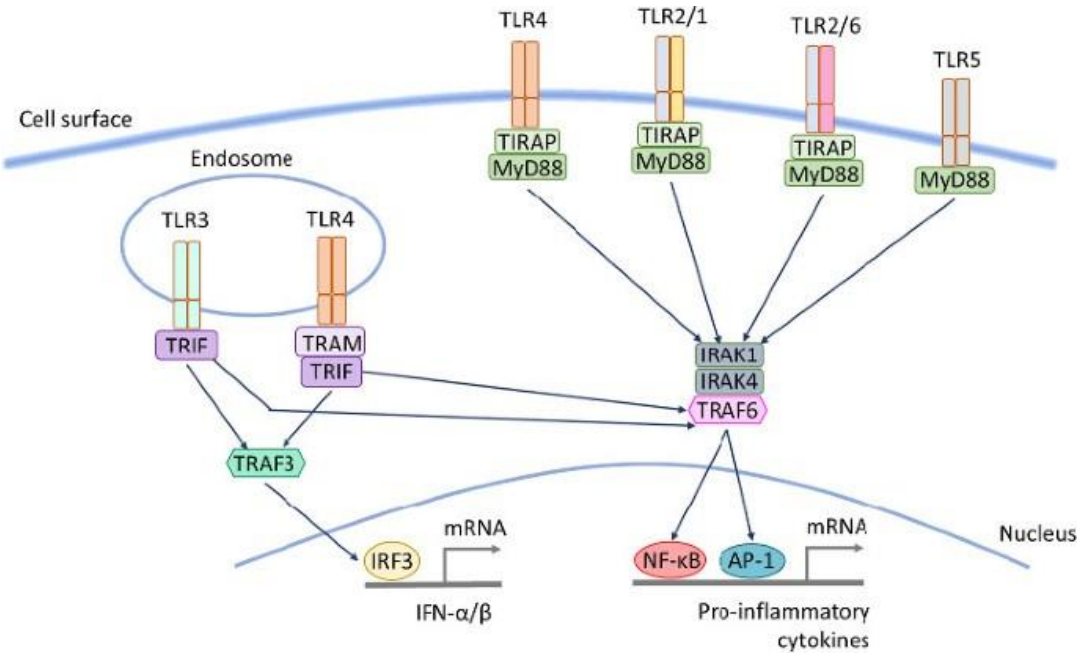

Figure 3 **Toll-like receptor signaling pathway** (from Laura A. McKiel 2020)

1.5 Recent Advances and Applications: Engineered Macrophages

Advances in biotechnology and genetic engineering have enabled the development of engineered macrophages with enhanced therapeutic potential, representing a promising frontier in cancer immunotherapy[92]. There are various strategies to manipulate macrophages, including genetic modifications to boost their cytotoxic functions, reprogramming to counteract immunosuppressive environments, and equipping them with novel receptors or therapeutic agents[93]. Recent studies have shown significant progress in utilizing engineered macrophages for cancer therapy, particularly in challenging solid tumors where traditional treatments often fall short.[94] In preclinical models and early clinical trials, these engineered macrophages have demonstrated substantial anti-tumor effects, effectively infiltrating tumors, modulating the tumor microenvironment (TME), and working synergistically with other immune cells to enhance the overall anti-tumor response[95]. Furthermore, combining engineered macrophages with other immunotherapies, such as checkpoint inhibitors, has shown synergistic effects that amplify the immune response and improve treatment outcomes.

1.5.1 Synthetic Receptor Therapies: CAR-Macrophages and SynNotch

1.5.1.1 CAR-Macrophages (CAR-M)

A breakthrough in the field of engineered macrophages involves the use of synthetic receptors, such as Chimeric Antigen Receptors (CARs), commonly known for their success in T-cell therapies. CAR are designed to recognize and target specific tumor antigens, allowing them to precisely attack cancer cells. CAR-M shares core components with CAR-T, including an extracellular domain that provides specific recognition through a single-chain variable fragment (scFv) of tumor-associated antigens such as CEA, CD19, and HER2[96,97]. Additionally, CAR-M includes a hinge domain, a transmembrane domain (CD64 or CD8), and an intracellular domain which enables specific downstream signalling pathways (e.g., CD3ζ and FcγR). Once a CAR-M recognizes a specific ligand, it triggers an intracellular signalling cascade, activating the macrophage (**Fig.4**). This leads to enhanced phagocytosis and secretion of pro-inflammatory cytokines like TNF-α and IL-12, which further recruit other immune cells, such as cytotoxic T-cells, to the tumor site [98]. Importantly, unlike CAR-T cells, CAR-M can modulate the tumor microenvironment by promoting the recruitment of additional immune effectors and transforming the TME from immunosuppressive to immunostimulatory.[99]

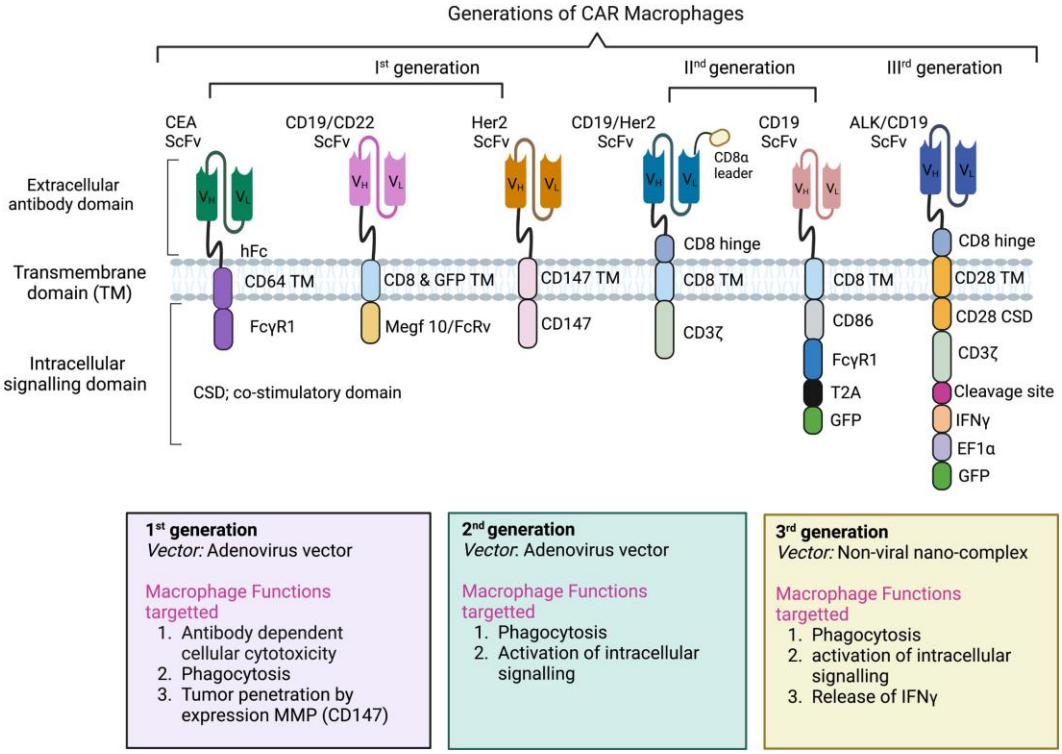

Figure 4 **CAR design for macrophages**. Each generation represents an improvement in the design of CARs, leading to enhanced efficacy and specificity in targeting cancer cells. (From Alok K. Mishra 2023)

1.5.1.2 SynNotch Receptors in Macrophages

Another innovative approach in the cell-based immunotherapy context involves the use of SynNotch, a customizable synthetic receptor system. SynNotch receptors allow for precise control over gene expression, enabling the macrophages to respond to specific cues in the TME. SynNotch receptors system is composed by[100] (**Fig.5**):

- **An extracellular sensing domain:** Recognizes a specific input signal (a tumor antigen or a particular cell surface marker).
- **A transmembrane domain:** Acts as a signal transducer.
- **An intracellular transcriptional module:** upon cleavage of the transmembrane domain, it acts as transcription factor that enters the nucleus and triggers the expression of genes regulating functions such as cytokine release, chemokine secretion, or phagocytosis activation.

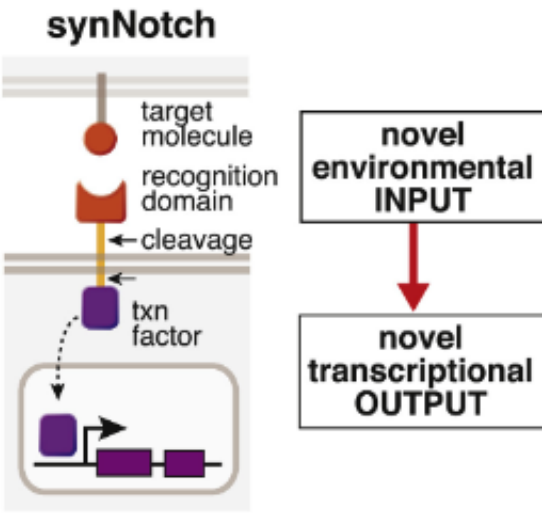

Figure 5 **Conceptual design of synNotch receptor systems (**from Leonardo Morsut 2016**)**

In the context of cancer, macrophages engineered with SynNotch receptors can be designed to activate a specific anti-tumor function only when they encounter their target, avoiding off-target effects and unwanted inflammation. For example, SynNotch can be programmed to express immune-activating cytokines or phagocytic enhancers upon encountering tumor cells, making this system particularly valuable in heterogenous TMEs where different regions of the tumor might express distinct molecular cues[101,102].

1.5.2 Genetic Modifications to Enhance Anti-Tumor Functions

1.5.2.1 CRISPR-Cas9-Based Genetic Engineering

One of the most exciting developments in the field of engineered macrophages is the use of genetic engineering tools like CRISPR-Cas9 to enhance the innate anti-tumor properties of these immune cells, allowing for precise genetic alterations that can either upregulate genes associated with macrophage activation or suppress genes that may contribute to their immunosuppressive functions. By utilizing CRISPR-Cas9, groups of researchers can knock out genes that contribute to macrophage immunosuppression, such as those involved in the upregulation of inhibitory receptors (e.g., PD-1 or SIRPα), or overexpress genes that enhance pro-inflammatory functions and anti-tumor activity (e.g., overexpression of TNF-α, IL-12, or specific chemokines like CCL2 to recruit additional immune cells). A particular focus has been the deletion of genes that favour an M2 phenotype (pro-tumor and anti-

inflammatory) and the reprogramming of macrophages towards an M1 phenotype (anti-tumor and pro-inflammatory)[103–105].

1.5.2.2 Delivery Mechanisms: Nanoparticles

Nanoparticles can be engineered to specifically target and reprogram tumor-associated macrophages (TAMs) within the tumor microenvironment (TME), offering a precise and effective therapeutic approach[106]. These nanoparticles, often composed of biodegradable materials like lipids or polymers, are designed to carry therapeutic agents such as small interfering RNA (siRNA), drugs, or plasmids. By loading nanoparticles with siRNA that targets transcription factors linked to the M2 macrophage phenotype, they can selectively knock down these factors in TAMs, promoting a shift toward the pro-inflammatory M1 phenotype. This approach enhances the anti-tumor activity of macrophages while minimizing off-target effects, improving the therapeutic efficiency[107]. Nanoparticles can also be modified with surface ligands that bind to receptors specifically expressed on TAMs, such as the mannose receptor or scavenger receptors, ensuring targeted delivery of their cargo directly to the macrophages in the TME[108]. Once internalized, the nanoparticles release their payload, enabling genetic reprogramming or the delivery of cytotoxic agents that enhance the macrophages' ability to kill tumor cells. This strategy represents a promising avenue for cancer therapy by exploiting the plasticity of macrophages and focusing therapeutic effects directly within the TME[109].

1.5.3 Enhancing Phagocytosis and Cytotoxicity

CD47 plays a pivotal role in immune evasion, allowing tumor cells to escape macrophage-mediated phagocytosis by engaging the SIRPα receptor and sending a 'don't eat me' signal. This axis is a critical mechanism by which many cancers evade the immune system, particularly macrophages, which are key components of the innate immune response[110]. By binding to SIRPα on macrophages, CD47 inhibits their ability to engulf and destroy tumor cells. Consequently, targeting this axis has become a promising strategy to reactivate the immune system to recognize and eliminate tumor cells. Anti-CD47 therapies have shown great potential in enhancing macrophage-mediated phagocytosis and promoting tumor elimination[111]. One of the most advanced therapies in clinical trials is Magrolimab, a monoclonal antibody that

directly targets CD47. By blocking CD47 interaction with SIRPα, Magrolimab[112] enables macrophages to overcome the inhibitory signal and attack the tumor. Early-phase clinical trials have demonstrated promising results, particularly in combination with other therapies, such as azacitidine for acute myeloid leukaemia (AML) and myelodysplastic syndromes (MDS), where patients have shown improved response rates. Another approach involves the use of ALX148[113], a fusion protein that blocks CD47 but avoids binding to red blood cells, reducing the risk of anaemia—a common side effect of systemic CD47 blockade. Despite the encouraging results, the systemic administration of these therapies can lead to off-target effects, particularly the depletion of red blood cells and platelets, which also express CD47. This has driven the need for more localized or targeted approaches to block CD47 and mitigate these side effects. The Kipp Weiskop [114] laboratory developed a SIRPα fragment with higher affinity for CD47 and reduced size compared to previous monoclonal antibodies, termed CV1. CV1 (SIRPα protein) fused to an Fc region of human IgG1 in Manfred Olfred's [115]laboratory demonstrated binding of the construct to CD47 present on MDA-MB-291 and reduced tumor growth in mouse models. Melita Irving's lab[116] combined the use of CAR-T cells with the release of the CV1 decoys protein so that its localized block not only reduces the risk of off-target toxicity but also improves macrophage phagocytosis directly at the tumor site. In addition, CV1 improves T cell-mediated cytotoxicity by allowing engineered CAR-T cells to persist in TME and kill cancer cells more effectively. However, expression of CD47 on CAR-T cells poses a risk of early cell depletion because CV1 can bind to the surface of CAR-T cells, making them susceptible to macrophage phagocytosis and thus reducing their persistence and long-term efficacy of treatment. The incorporation of the CV1 in CAR-T cell therapy presents a promising approach for improving tumor control by targeting the CD47 checkpoint.

1.5.4 Reprogramming Macrophages to an M1 Phenotype

Recent advances in cancer immunotherapy have highlighted the critical role of the TME in determining therapeutic outcomes, particularly through the modulation of immune cells like macrophages. Macrophages within tumors often adopt an immunosuppressive M2 phenotype, supporting tumor growth and metastasis. However, through targeted activation of Toll-like receptors (TLRs), macrophages can be repolarized to an M1 phenotype, which is characterized by enhanced pro-inflammatory and anti-tumor activity[83]. TLRs, particularly TLR4 and TLR5, are pivotal in recognizing bacterial components and initiating immune responses[86].

[redacted]

. Similarly, NAP-armed CAR T cells harness TLR pathways to overcome the immunosuppressive tumor microenvironment in solid tumors[118]. By secreting NAP, these engineered CAR T cells attract and activate neutrophils, dendritic cells, and macrophages, fostering an immunologically "hot" environment that facilitates not only the destruction of tumor cells directly targeted by CAR T cells but also the recruitment of bystander T cells through epitope spreading. This broad immune activation addresses the challenge of antigen heterogeneity within tumors, which often impedes the success of conventional therapies. Together, these approaches underline the potential of bacterial proteins in modulating TLR-mediated pathways to reprogram the tumor microenvironment, shifting it from immunosuppressive to immune-active, thereby improving the efficacy of cancer immunotherapy.

2 Aim of study

This study presents a synthetic biology approach to develop a macrophage-based immunotherapy, to improve current T cell therapies and address the challenges posed by their use in solid cancers. It aims to address two fundamental limitations of existing immunotherapies: i) the localized administration of therapeutic agents in the tumor microenvironment (TME), and ii) the precise regulation of therapeutic molecular expression. The overarching goal is to design macrophages with a synthetic system composed of a sensor module (SynNotch) that can detect specific targets in the TME conditions (such as cancer cells, T-cells, and chemokines) with an actuator module (secreted therapeutic agents) that promote phagocytosis and macrophage repolarization from an M2 phenotype to a M1 phenotype. By allowing macrophage repolarization and enhanced phagocytosis in a controlled and targeted manner, this strategy offers a new way to develop more precise and effective cancer immunotherapies. While the development of the sensing part, based on the SynNotch system was carried out by a Postdoc in Siciliano lab, my work focused on the characterization of potential actuators.

2.1 Aim 1: Increased phagocytosis of cancer cells (First Actuator)

CD47-targeting antibodies, while promising as a therapeutic strategy in cancer treatment due to their ability to block the "don't eat me" signal and promote tumor cell phagocytosis, are associated with several potential side effects. One major concern is the off-target effect on healthy cells, particularly red blood cells (RBCs), which express CD47 at high levels[119]. This can lead to unintended phagocytosis of RBCs, resulting in anaemia and related complications[120]. Additionally, the widespread expression of CD47 on various tissues raises concerns about possible immune-related toxicities, such as neutropenia and thrombocytopenia[121]. Recent advancements in antibody engineering aim to reduce these side effects by improving the specificity and minimizing the impact on non-cancerous cells.

To enhance the specificity of CD47-targeting antibodies and mitigate side effects, we aimed to engineer macrophages with a sensor-actuator system incorporated into a lentiviral platform. As actuator module, we utilized a mutated version of the N-terminal V-set immunoglobulin (Ig) domain of SIRPα, known as CV1 consensus

(residues 1 to 118) fused to an Fc region of human IgG1 from Manfred Ogrif's [115]lab, which enhances the phagocytosis of cancer cells. This actuator is positioned under the control of a sensor module (SynNotch) that becomes activated exclusively in the presence of a ligand enriched in the TME, allowing for the controlled release of the SIRPα protein and thereby reducing off-target effects on healthy tissues.

2.2 Aim 2: Re-polarization from M2 to M1 phenotype (Second Actuator)

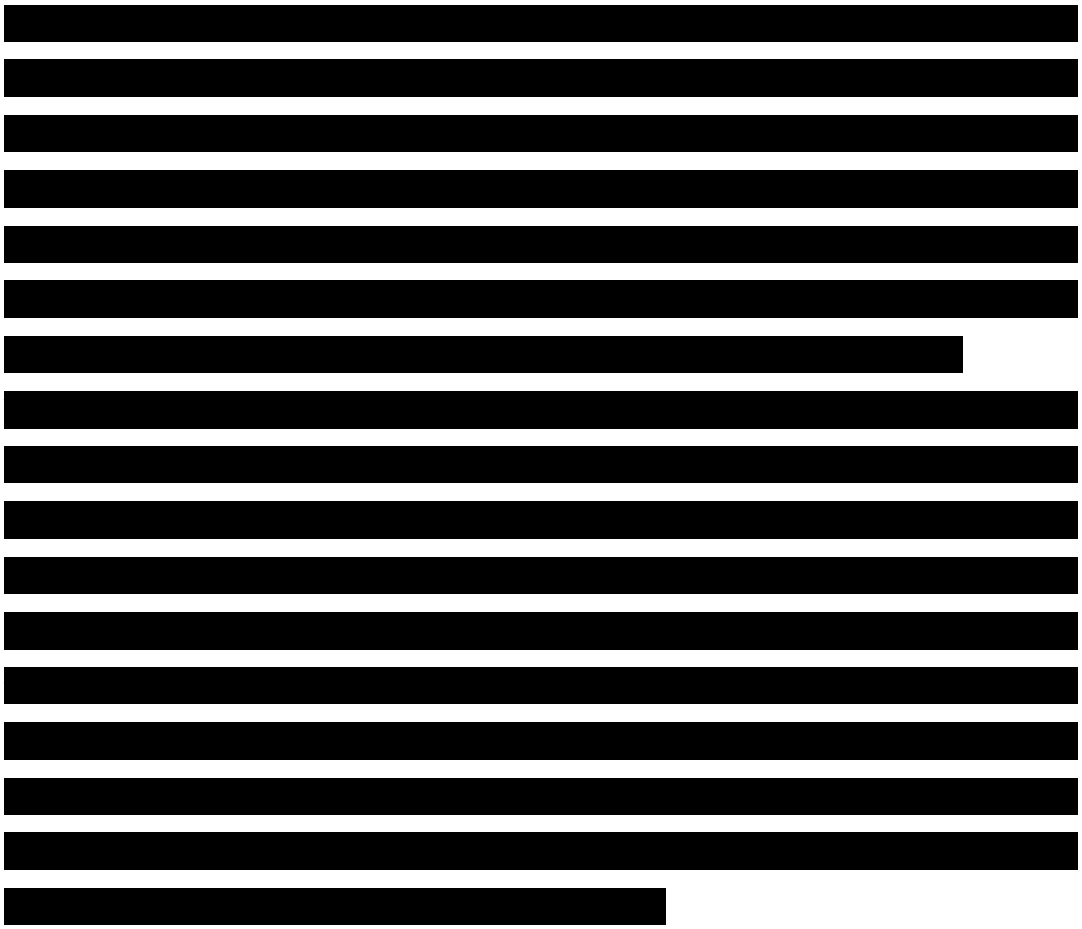

3 Materials and Methods

3.1 Lentiviral Vector cloning

3.1.1 MTK Assembly

The Mammalian ToolKit (MTK) is a Golden Gate-based cloning toolkit for fast, reproducible, and versatile assembly of large DNA vectors and their implementation in mammalian models. The MTK consists of a curated library of characterized, modular parts that can be assembled into transcriptional units and further weaved into complex circuits[123].

MTK allows the cloning of multiple transcription units (TU). In our case, the first step is represented by domestication in a standard vector using a Type II restriction enzyme (Esp3I). SIRPα-Fc was cloned by PCR from a template plasmid from the Manfred Ogrif's lab [115] and BC was instead ordered as a DNA string. The second step is represented by the assembly of the domesticated TUs into Ampicillin-resistant vectors using a BsaI Golden Gate assembly.

3.1.2 In-Fusion HD Cloning

In-Fusion Cloning Kit (Takara Bio USA) allows one-step cloning of one or multiple fragments into any vector. The cornerstone of In-Fusion cloning technology is the In-Fusion Enzyme, which chews back the 3' end of each DNA strand and allows the pairing of the complementary DNA fragments (e.g., PCR-generated inserts and linearized vectors) efficiently and precisely by recognizing 15-bp overlaps at their ends (Bio USA Inc, n.d.). For the Infusion protocol a ratio of backbone to insert of 1:2 was used. The Infusion Cloning was performed in a 10 µl reaction volume which includes: the LV vector (pHR UAS backbone was a kind gift from the Roybal lab[124]) previously linearized with restriction enzymes (BamHI and EcorI), PCR-generated insert, the 5X In-Fusion HD Enzyme, and finally H2O up to the final volume. The assembly was performed accordingly to the manufacturer's protocol.

The obtained plasmids were then used as transfer plasmids for lentivirus production (see 3.2.8). Schemes of final LVs were shown in **Fig 8 e Fig 15.**

3.1.3 Bacterial transformation and culture

For Domestication parts: 20 ul of competent cells (NEB® Stable Competent E. Coli High Efficiency, C3040H) are transformed with 2 ul of GoldenGate product. After thawing them on ice, the GoldenGate product is added to the cells, and they are incubated 5' on ice. Following theis incubation, e. SOC medium (Clontech) is added and bacteria and grow for 1h at 37°C after are plated on plates with Cloranphenicol, thus allowing the bacteria selection through the CMP resistance gene present into the backbone.

Cells undergo an outgrowth at 37°C 12h to reduce recombination. After 12h green colonies as considered as negative control, and some of the white colonies undergo a further outgrowth in liquid LB.

For In-Fusion: Bacterial transformations used Stellar Competent Cells (TAKARA). An aliquot of cells was thawed on ice and 30 µL of cells were mixed with roughly 2 µL of In-Fusion reaction and then were left for 35 minutes on ice. Heat-shock was performed by incubation for exactly 45 seconds at 42°C in a dry heat block and placed for 2 minutes on ice. All transformations underwent an outgrowth step in SOC Medium (Clontech) with incubation in a shaking incubator (30°C, 200 rpm) for 24h. . Plasmid purifications were done according to the manufacturer's instructions using E.Z.N.A.® Plasmid Mini Kit I (VWR), QIAGEN Plasmid Plus Kit, and QIAGEN Plasmid Plus Maxi Kit. All plasmids were verified by Sanger sequencing

3.2 In vitro characterization

3.2.1 Cell culture

HEK293T-17, SKOV3, MDA-MB-231, A549 cells (ATCC) used in this study were maintained in Dulbecco's modified Eagle medium (DMEM, Gibco) supplemented with 10% heat-inactivated Fetal Bovine Serum (FBS non-USA origin, Sigma-Aldrich), 1% penicillin/streptomycin (Sigma-Aldrich), 1% L- Glutamine (Sigma-Aldrich) and 1% MEM non-essential amino acids (Sigma-Aldrich). THP-1, Jurkat and Raji cells (ATCC), THP-1 [redacted]) were cultured in RPMI-1640 supplemented with 10% of FBS, 1% penicillin/streptomycin (Sigma-Aldrich), 1% L- Glutamine (Sigma-Aldrich) and 1% MEM non-essential amino acids (Sigma-Aldrich). Adherent Cells were detached by incubation with Trypsin-EDTA phenol

red solution (Sigma-Aldrich) for 5 minutes at 37°C. While THP1 when differentiated to macrophages detach with Accutase (Sigma-Aldrich) for 10 minutes at 37°C. All the cell lines were maintained at 37°C in a 5% CO2-humidified incubator.

3.2.2 Primary Monocyte Isolation

Buffy coats from healthy anonymous donors were received from the blood transfusional center of the "University Hospital-Federico II" of Naples or from the blood transfusional center of the San Paolo Hospital of Naples. PBMCs are isolated by blood through density gradient centrifugation via Ficoll Paque Plus (Sigma-Aldrich, GE17-1440-02). Blood is diluted 1:1 with Dulbecco's Phosphate Buffered Saline (PBS) (Sygma-Aldrich, D8537), and stratified on Ficoll Paque Plus in a ratio Blood: Ficoll=1: 1.5, considering the volume of the blood before the dilution. After centrifugation (30', 400g, RT) with no brake and accelerator, PBMCs stratify between plasma, containing platelets, and FICOLL, containing granulocytes. They are collected and washed in PBS with a ratio PBMCs: PBS=1:3 with a centrifugation (10', 150g, RT). Pelleted cells are resuspended in PBS and counted via Trypan Blue 0.4% (Gybco), using a strong dilution, due to the large number of cells. They are centrifuged (10', 150g, RT) and resuspended in homemade MACS buffer composed by PBS, Bovin serum Albumin (BSA) 0.5% (Sygma-Aldrich, A2153), EDTA (Sygma-Aldrich, T 3924) 2mM.

Primary monocytes are isolated via negative selection using a "Classical Monocyte Isolation Kit, human" (Milteny Biotec 130-117-337) according to the manufacturer's instructions. The magnetic isolation is performed. LS column (Miltenyi Biotec,130-042-401) is placed in the magnetic field of the MACS separator (Miltenyi Biotec, 130-042-303). CD14+ cells are counted are resuspended in RPMI-1640 (Life Technologies, 21875091) supplemented with 10% of FBS, 1% penicillin/streptomycin (Sigma-Aldrich), 1% L- Glutamine (Sigma-Aldrich) and 1% MEM non-essential amino acids (Sigma-Aldrich), Human M-CSF (Life Technologies italia) at the final concentration of 25ng/mL..

3.2.3 Monocyte differentiation into macrophages

CD14 cells were plated on p100 tissue culture plates at a density of 30.000.00 cells/cm^2 in RPMI-1640 medium supplemented with 25ng/mL M-CSF. Replace half of the media every 3 days. CD14+ differentiated into Macrophages after 6–7days (M0). M0 macrophages were detached with Accutase (Product #A6964-100ML, Sigma-Aldrich) and were then polarized to M1 or M2 macrophages for 24h and 48h in RPMI-1640 medium supplemented with: 10ng/mL LPS and 20 ng/mL IFN-γ for M1; 20 ng/m IL-4 and 20ng/ml IL13 for M2. To mimic a condition that simulated the tumor microenvironment we created in the laboratory a Conditioned Medium [redacted]

3.2.4 Monocyte differentiation in the presence of Bacterial Compound (BC)

CD14$^+$ cells were plated on p100 tissue culture plates at a density of 30.000.00 cells/cm2 in RPMI-1640 medium supplemented with 25ng/mL M-CSF. Replace half of the media every 3days. CD14+ differentiated into Macrophages after 6–7days (M0). M0 macrophages were detached with Accutase (Product #A6964-100ML, Sigma-Aldrich) and seeded in 96well plate at density of 100.000cells were then polarized to M1 or M2 macrophages for 24h and 48h in RPMI-1640 medium supplemented with different stimuli: 10ng/mL LPS and 20 ng/mL IFN-g for M1; 20 ng/m IL-4 and IL13 20ng/ml for M2. After 24h of polarization, added the medium from HEK-293T transfection with BC protein with refresh stimuli. Expression of CD80 and CD206 in macrophages was measured by FACS after 48h of polarization.

3.2.5 THP-1 Differentiation into macrophages

THP-1 polarization was performed in different plate formats depending on experimental requirements. Plated on 6well or 12well or 24well tissue culture plates respectively at a density of $5x10^5$- $4.2x10^5$- $2.5x10^5$ cells/cm^2 in RPMI 1640 with PMA at a final concentration of 10nM for 48h. After 48h THP-1 cells differentiate into Macrophages (M0). After 48h removed the PMA and M0 macrophages were then polarized to M1 or M2 macrophages for 24h and 48h in RPMI-1640 medium

supplemented with different stimuli: 10ng/mL LPS and 20 ng/mL IFN-g for M1; 20 ng/m IL-4 and IL13 20ng/mL for M2. To mimic a condition that simulated the tumor microenvironment we created in the laboratory a conditioned medium [redacted]

3.2.6 THP-1 Differentiation in the presence of Bacterial Compound

THP-1 polarization was performed in 24well tissue culture plates respectively at a density $2.5x10^5$- in RPMI 1640 with PMA at a final concentration of 10nM for 48h. After 48h THP-1 cells differentiate into Macrophages (M0). After 48h removed the PMA and M0 macrophages were then polarized to M1 or M2 macrophages for 24h and 48h in the SN from HEK-293T transfected that contain BC protein secreted supplemented with different stimuli: 10ng/mL LPS and 20 ng/mL IFN-g for M1; 20 ng/m IL-4 and IL13 20ng/ml for M2. Expression of CD80 and CD206 in macrophages was measured by FACS after 24h and 48h of polarization.

3.2.7 Cell transfection

HEK293T-17 cell line was transfected in all experiments with PEI® transfection reagent (Polysciences) according to manufacturer's instructions, using a ratio DNA (µg): PEI (µl) =1:3. Transfections were performed in different plates or T25 or T75 Flask depending on experimental requirements. For harvesting of CV1-Fc protein medium for competition assays, phagocytosis or for BC protein production, HEK293T-17 cells were transfected in T25 or T75 Flask. Cells were seeded at 2x10^6 cells or 5x10^6 per well in a final volume of 6 or 14 ml. The day before were transfected by PEI® using 3µg of total DNA or 10µg. Transfected cells were analyzed in flow cytometry after 48 hours to observe the expression of protein, and the cell medium was stored at -80°C to perform competition assay (CV1-Fc) and re-polarization (BC).

3.2.8 Lentivirus production

Second-generation lentiviral vectors were produced by transfection of HEK293T-17 with transfer plasmid and the two packaging vectors. Briefly, HEK293T-17 cells were seeded at $5x10^6$ in a total volume of 15mL of DMEM complete medium in a T75 flask. The Day after, cells were transfected with a mix containing 7.5 µg of transfer plasmid (CV1-Fc plasmids) 3.75µg of pMD2.G (Plasmid #12259, Addgene) and 3.7 µg of psPAX2 (Plasmid #12260, Addgene) using FuGENE HD Transfection Reagent using a ratio DNA: FuGene=1:3 (Product # E2311, Promega). After 10h of transfection change the media to remove FuGene. The viral supernatant was harvested at 48h and 72h post-transfection, 0.45 µm filtered, divided in aliquots and stored at -80°C until use.

3.2.9 Lentivirus Titer

Lentivirus titrations were carried out directly in THP-1 cells in 24-well plates.
Lentivirus was added to cells at the dilution of 1:300; 1:600; 1:900.
After 7 days the LNGFR and Myc-Tag was measured by flow cytometry and based on the samples with a percentage of fluorescence of 20-40% titer was calculated with this formula:

$$\frac{T = N * F * D}{VT}$$

where T = Titer, TU/mL; N = Number of cells transduced; F = Fraction of cells with fluorescence; D = Dilution Factor; VT = Transduction Volume, mL (see "GTA for Functional LV Quantification")

3.2.10 Cell Transduction

THP-1 cells were engineered with CV1-Fc constructs by lentiviral transduction. Briefly, transductions were performed in 24well plates seeding 300.000 cells per well in growth medium. Cells were infected with different dilution in the presence of Polybrene (Sigma-Aldrich) at a final concentration of 10 µg/ml to enhance transduction efficiency. 2 days after, LV-containing medium was removed, and fresh medium was added. Then, cells were usually split 48 hours after transduction.

Transduction efficiency was assessed 7 days post-transduction by LNGFR/ Myc-Tag staining. (see 4.2.5.1).

3.2.11 In vitro co-culture of THP-1 engineered cells and Jurkat cells

3.2.11.1 In Suspension

To detect the activation of the circuit, perform a suspended co-culture of engineered THP1 with Jurkat with and without ligand. Seeding in suspension THP-1: Jurkat at a ratio of 1:3 (50,000 cells THP-1 and 150,000Jurkat). After 48h of Co-culture perform a FACS analysis to observe the expression of the protein eBFP as shown in paragraph 4.2.5.2

3.2.11.2 In Adhesion

To detect the activation of the adhesion circuit, co-cultured in THP1 engineered with Jurkat cells with and without ligand. Seed 480.000 THP1 cells in the 24well plate. After 2 days detach the THP1 with Accutase, add the different polarizing stimuli to induce M1-M2. At the same time collect the Jurkat cells with and without ligand (400.000 x 3), perform staining with CFSE CellTrace™ CFSE Cell Proliferation Kit, for flow cytometry (Product # C34554, **Thermo Scientific**) and co-culture with the macrophages. After 48h, perform analysis at FACS to observe both eBFP expression protein and Phagocytosis.

3.3 Actuators Characterization

3.3.1 Flow cytometry

Extracellular staining

For phenotype markers and receptors of phagocytosis, cells treated in 6well plates were washed with DPBS (Thermo Fisher), detached with 500uL of Accutase® solution,sterile-filtered, suitable for cell culture (Product # A6964-100ML, Sigma-Aldrich) and re-suspend in 1mL of medium. Cells were washed with DPBS and were labelled with **Fc Receptor** Binding Inhibitor Polyclonal Antibody (Product # 14-9161-73, Invitrogen), for 15minutes at room temperature. After labelled with

markers of phenotype with 0.2ug of CD80 (B7-1) Monoclonal Antibody (2D10.4), Super Bright™ 702 (Product #67-0809-42, Biolegend) CD169 (Siglec-1) Monoclonal Antibody (7-239), PE-eFluor 610 (Product # 61-1699-42, Biolegend), CD64 conjugated PerCP/Cyanine5.5 (Product # 305024, Biolegend), CD206 conjugated BV421 Mouse Anti-Human (Product # 564062, Biolegend), and receptor of phagocytosis LILRB1 CD85j (ILT2) Antibody conjugated FITC (Product # 333730, Biolegend), SIGLEC10 conjugated PE/Cyanine7 (Product # 347608, Biolegend), SIRPα (CD172a) conjugated PE anti-human (Product # 372104 , Biolegend) in a final volume of 50uL of Brilliant Buffer for 20 minutes at room temperature.

For ligand of cancer cells, I used 250.000 cells for the staining. Were washed with DPBS (thermo Fisher). Cell suspension was divided in three for antibody, isotype control and unstained conditions. Cells were washed in DPBS and were labeled with 0.2 μg CD47 Monoclonal Antibody (B6H12) FITC (Product # 11-0479-41 , Biolegend), MHCI anti-human HLA-A,B,C Brilliant Violet 510™ (Product #311435, Biolegend), CD24 Antibody Anti-Human conjugated Brilliant Violet 711 (Product # 311135, Biolegend) in a final volume of 50 ul DPBS for 20 minutes at room temperature.

For competition assay, cells treated in 24-well plates were washed with DPBS (Thermo Fisher), detached with 200 μL of Accutase® solution,sterile-filtered, suitable for cell culture (Product # A6964-100ML, Sigma-Aldrich) and re-suspended in 500μL of medium. Cell suspension was divided in three for antibody, isotype control and unstained conditions. Cells were washed in DPBS and were labeled with 0.2 μg of anti CD47 FITC Antibody (Product # 11-0479-42, Biolegend) or 0.2 μg of Mouse IgG1 kappa Isotype Control, FITC in a final volume of 50 ul DPBS for 20 minutes at room temperature.

For the analysis of LNGFR$^+$ population and MycTAG, seven days after the transduction cells were washed in DPBS Cells were washed with DPBS and were labelled with Fc Receptor Binding Inhibitor Polyclonal Antibody (Product # 14-9161-73, Invitrogen), for 15minutes at room temperature. After were stained with Pacific Blue™ anti-human CD271 (NGFR) Antibody (Product #345132, Biolegend) and Myc-Tag (9B11) Mouse mAb (PEConjugate) (Product #3739, Cell Signaling) for 20 minutes at room temperature. After antibody incubation, cells were washed in

DPBS, resuspended in 180 ul of FACS buffer and analyzed by using a BD FACS Celesta Cell Analyze.

For Maturation of Macrophages, to detect whether the primary monocytes have become mature macrophages we used anti-human CD14 conjugated Brilliant Violet 510 (Product #301842, Biolegend). To detect whether the THP-1 have become mature macrophages we used anti-human CD11b conjugated PE/Cyanine5 (Product # 301308, Biolegend)

3.3.2 CD47 Competition Assay

For competition assay HEK293T-17 cells were seeded at $5x10^6$ cells in T75 in a final volume of 16ml. The day before cells were transfected by PEI® transfection reagent using a ratio DNA: PEI=1:3 (Polysciences) and plate MDA-MB-231 or SKOV3 cells were seeded respectively at 70.000 cells and 40.000cells per well in 24-well plate in a final volume of 0.5ml. For Jurkat cells being in suspension, the same day of the competition test 400,000cells are placed in the 24well. After 48 hours tumor cells were treated with 0.5ml of transfected HEK293T-17 supernatant for 1 hour at 37°C in a 5% CO2-humidifed incubator. The remaining supernatant of transfected cells was harvested and stored at -80°C for further experiments. Cells not treated with HEK293T-17 supernatants were used as untreated (UT) control. Afterwards, tumor cells were stained with anti CD47 mAb (as described in section 4.2.3 and 4.2.5.2 **fig 12c**).

3.3.3 Phagocytosis assay

To detect the CV1-Fc functionality with medium collected from HEK-293T: M0 macrophages were plated into 12-well plates at a density of 420,000 cells/well and cultured in RPMI. After 2 days the differentiation is induced by different polarization stimuli. After 24h and 48h of polarization Jurkat tumor cells were prepared at ratio 1:3 (macrophage/Cancer cells) and stained with CFSE CellTrace™ CFSE Cell Proliferation Kit, for flow cytometry (Product # C34554, **Thermo Scientific**), 1uL of solution into 1mL of DPBS. Jurkat cells were incubated for 20min at 37°C. After 4 volumes of RPMI was added and put for another 5min at 37°C. The cell suspension was then centrifuged at 300g for 5 min, and the supernatant was removed, followed

by gently resuspending the cells in warm (37°C) medium. The washing procedure was repeated two more times. The CFSE labeled Jurkat cells were resuspend in the SN from TF of HEK-293T that contain CV1-Fc protein and seeded onto the macrophages. The cells were incubated at 37 °C for 3 h. Each well was washed with DPBS, and macrophages were dissociated with Accutase and stained with CD11b antibody. Fluorescence intensity of CFSE in macrophages was measured by FACS after 24h and 48h of polarization

To detect the Functionality of CV1-Fc in the Sensor/ Actuator system: M0 macrophages were plated into 12-well plates at a density of 420,000 cells/well and cultured in RPMI. After 2 days the macrophages were detached, the differentiation is induced by different polarization stimuli. Jurkat with and without ligand were prepared at ratio 1:3 (macrophage/Cancer cells) and stained with CFSE CellTrace™ CFSE Cell Proliferation Kit, for flow cytometry (Product # C34554, Thermo Scientific), 1uL of solution into 1mL of DPBS. Jurkat cells were incubated for 20min at 37°C. After 4 volumes of RPMI was added and put for another 5min at 37°C. The cell suspension was then centrifuged at 300g for 5 min, and the supernatant was removed, followed by gently resuspending the cells in warm (37°C) medium. The washing procedure was repeated two more times. The CFSE labeled Jurkat with and without ligand seeded onto the macrophages. The cells were incubated at 37 °C for 48h of polarization. Each well was washed with DPBS, and macrophages were dissociated with Accutase and stained with CD11b antibody. Fluorescence intensity of CFSE in macrophages was measured by FACS after 48h of polarization.

3.3.4 ELISA Assay

TNF-α and IL6 release from human cells was measured using the Lumit™. Lumit™ TNF-α (Human) Immunoassay (Product # W6050, Promega) and Lumit™ IL-6 (Human) Immunoassay (Product # W6030, Promega), respectively, as for the manufacturer's instructions. Briefly, the immunoassays use two antibodies directed against TNF-α and IL6 that are labelled with either the small, 11-amino acid subunit of NanoBiT® Luciferase (SmBiT) or the complementary 17.6 kDa subunit (LgBiT). When the labelled antibodies are brought into proximity due to binding to IL-1β and substrate is added, reconstituted NanoBiT® luciferase generates a bioluminescent signal proportional to analyte levels. The assays are performed with

frozen supernatant after re-polarization protocol. A mixture of the Lumit™ TNF-α and IL6 antibodies were incubated with the cells for 1h, followed by addition of the Lumit™ detection reagent. Luminescence was recorded on a GloMax® Discover luminometer.

3.3.5 SEAP assay

To determine if BC proteins activate NF-κB, THP1-[redacted] were treated with SuperNatant (SN) (that contain BC protein) collected from HEK-93T transfection. Subsequently, the supernatants that contain BC protein were harvested.and analyzed to determine if NF-κB was activated. The QUANTI Blue assay (rep-qbs, InvivoGen;San Diego, CA) was used to determine the level of secreted alkaline phosphatase (SEAP) reporter protein in the macrophage supernatants which correlates with NF-κB activation. The assay was performed according to the manufacturer's protocol. Briefly, 180 μL aliquots of QUANTI-Blue solution and 20 μL of macrophage supernatants from the various treatments were mixed in wells of a flat-bottom 96-well plate. The plate was then incubated for 3 h at 37 ˚C. Subsequently, the 620 nm optical density of the solutions in each well was determined with InSpire machine. The optical density correlates with the level of SEAP in the solution and thus the level of NF-κB activation.

3.3.6 Statistics

Data were analyzed and plotted with Biorender. The statistical test used is a two-tailed paired student t-test. Statistical significance was determined using the methods described in the results section or in the figure legends.

4 Results

4.1 In vitro model of macrophage polarization

To be able to test the efficacy of our synthetic circuits in terms of macrophage polarization, we optimized and validated previously published protocols on in vitro polarization using THP-1 cells as source of monocyte-like cells and primary monocytes $CD14^{+}$[,125,126]. For inducing the maturation of the THP1 cells to macrophages M0 we treated cells with phorbol-12-myristate-13-acetate (PMA) for 48 hours. Then interferon (INFy) and Lipopolysaccharide (LPS) were added to stimulate the M1 phenotype, whereas IL4 and IL13 were used to induce the M2 phenotype (**Fig. 6a**). To mimic the formation of TAMs *in vitro*, we cultured THP-1 cells with conditioned medium (CM) collected from cancer cell lines SKOV3 (Ovarian cancer)[127] with IL4, IL13, IL10, and TGFβ were added to cancer cells CM (conditioned medium), diluted 1:1 with RPMI complete[,128] . The SKOV3 cell line were also chosen for the high expression of CD47 reported in the literature[129]. Phenotypical analysis was carried out by flow cytometry 24 and 48 hours after the addition of the cytokines to test the expression of phenotypic markers of the M1 (CD64-CD169-CD80) and M2 (CD206) states.

In parallel, to obtain mature human macrophages, we isolated $CD14^{+}$ cells from peripheral blood mononuclear cells (PBMCs) (**Fig. 6b**). PBMCs, which include $CD8^{+}$ and $CD4^{+}$ T lymphocytes, monocytes, and dendritic cells, can be isolated from healthy donors through density gradient centrifugation. Primary $CD14^{+}$ monocytes are selected using negative magnetic separation. During this process, PBMCs pass through a magnetic column, where all antibody-bound cells - including activated $CD8^{+}$ and $CD4^{+}$ T lymphocytes, platelets, red blood cells, and NK cells - are retained. $CD14^{+}$ cells, which remain unbound, are eluted, collected, and plated in the presence of macrophage colony-stimulating factor (M-CSF). The medium was partially changed every 3 days. After 7 days in culture, mature macrophages are obtained, and polarization is induced in vitro by adding a cytokine cocktail specific to each phenotype as described above. After 24 and 48 hours of differentiation, analysis was performed using flow cytometry to test the expression of phenotypic markers of the M1 (CD169) and M2 (CD206) states.

In the THP-1 model, we observed that CD64, CD169 and CD80 markers had the highest expression in the M1 state as expected. Conversely, CD206 marker was highly expressed in M2 and CM (**Fig. 6c**). For the primary monocyte model, CD169 had the highest expression in the M1 state as expected both at 24h and 48h post-treatment. Higher expression of CD206 in the M2 phenotype is clearly observed after 48h (**Fig. 6d**). These results suggest that the polarization of the THP-1 and primary monocyte cells to M1 and M2 states *in vitro* worked. For this reason, we can test the efficacy of the synthetic circuit we designed on different macrophage states in the context of the *in vitro* models we validated.

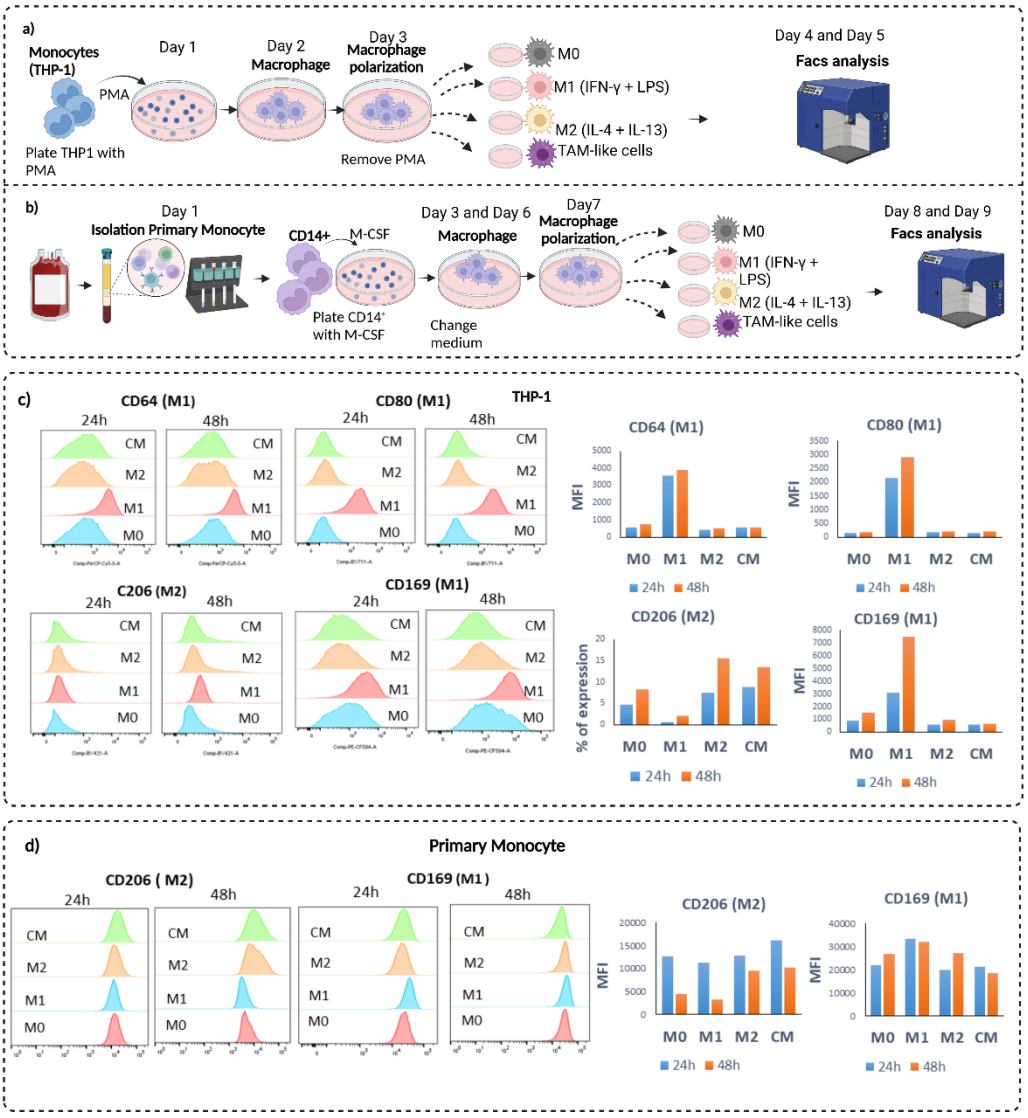

Figure 6 **a) Schematic representation of the experimental workflow that leads to THP-1 polarization**. PMA was added to THP1 cells for 48h, followed by polarization in phenotypes M1 and M2. 24-and 48-h post-polarization we analyzed the results by flow cytometry **b)** Polarization of **primary monocyte isolated from peripheral blood**. PBMCs are isolated from

buffy coats of blood donors through a density gradient centrifugation. CD14+ are isolated via negative selection and grown in the presence of Macrophage colony-stimulating factor *(*M-CSF). Media was changed every 3 days in 1:1 ratio old-new media for 7 days when a complete maturation of macrophages at the state M0 is obtained. Next, we added the cytokine cocktail for the induction of the phenotype M1 and M2 **c)** Representative histograms of one experiment (N=2). 24 hours and 48 hours after polarization the cells were analyzed by flow cytometry. for CD169-CD64-CD80 the median fluorescence intensity is observed while for CD206 the percentage of expression is compared. **d)** Representative histograms of one experiment (N=2). 24 hours and 48 hours after polarization the cells were analysed by flow cytometry. for CD169-CD64-CD80 the median fluorescence intensity is observed while for CD206 the percentage of cells expression is compared

4.2 Characterization of therapeutic actuator 1

4.2.1 Characterization of the receptors and ligands involved in "don't eat me" signals

Once the functionality of our in vitro model was confirmed, we evaluated by flow cytometry the expression of markers involved in the phagocytosis axis CD47, MHC I, and CD24 ligands (**Fig. 7a**) in cancer cell lines that grow both in adhesion and suspension, namely breast cancer cells MDA-MB-231, ovarian tumor cell line SKOV3, lung cancer cell A549, leukemia tumor cells Jurkat and lymphoblastic cancer cells Raji (**Fig. 7b**). CD47 is highly expressed on SKOV3, MDA-MB231, and Jurkat cell lines (**Fig.7b)**. SKOV3 also shows a high level of expression of CD24, and MHC-I compared to other cell lines. In parallel, I compared the expression levels of SIRPα, LILRB1 and SIGLEC10 receptors on the surface of the macrophage in different polarization states (M0-M1-M2-CM) after 24 and 48 hours of treatment with cytokines. After polarization, THP-1 exhibited high levels of SIRPα regardless of the phenotypic state (**Fig.7c**); LILRB1 showed a higher expression in the M1 phenotype whereas SIGLEC10 positive cells increased in the M2 and CM phenotypes (**Fig.7c**). Similar to THP-1, also in the primary monocyte model, SIRPα resulted highly expressed in all tested conditions after 24h and slightly less expressed after 48h in the M1 state. LILRB1 showed a robust expression in the M2 phenotype after 24h and in CM especially after 48h, while SIGLEC10 expression progressively increased between different phenotypes after 48h, especially in M2 e CM (**Fig.7d**). Collectively, these results suggest that SKOV3, MDA-MB231, and Jurkat cells are good candidates as cancer models to study the SIRPα-Fc actuator,

given the high expression of CD47. The receptors expression panel on macrophages indicate their levels of expression in different phenotypes within a tumor microenvironment (TME) serving as the basis for more detailed future studies on the other axes of phagocytosis.

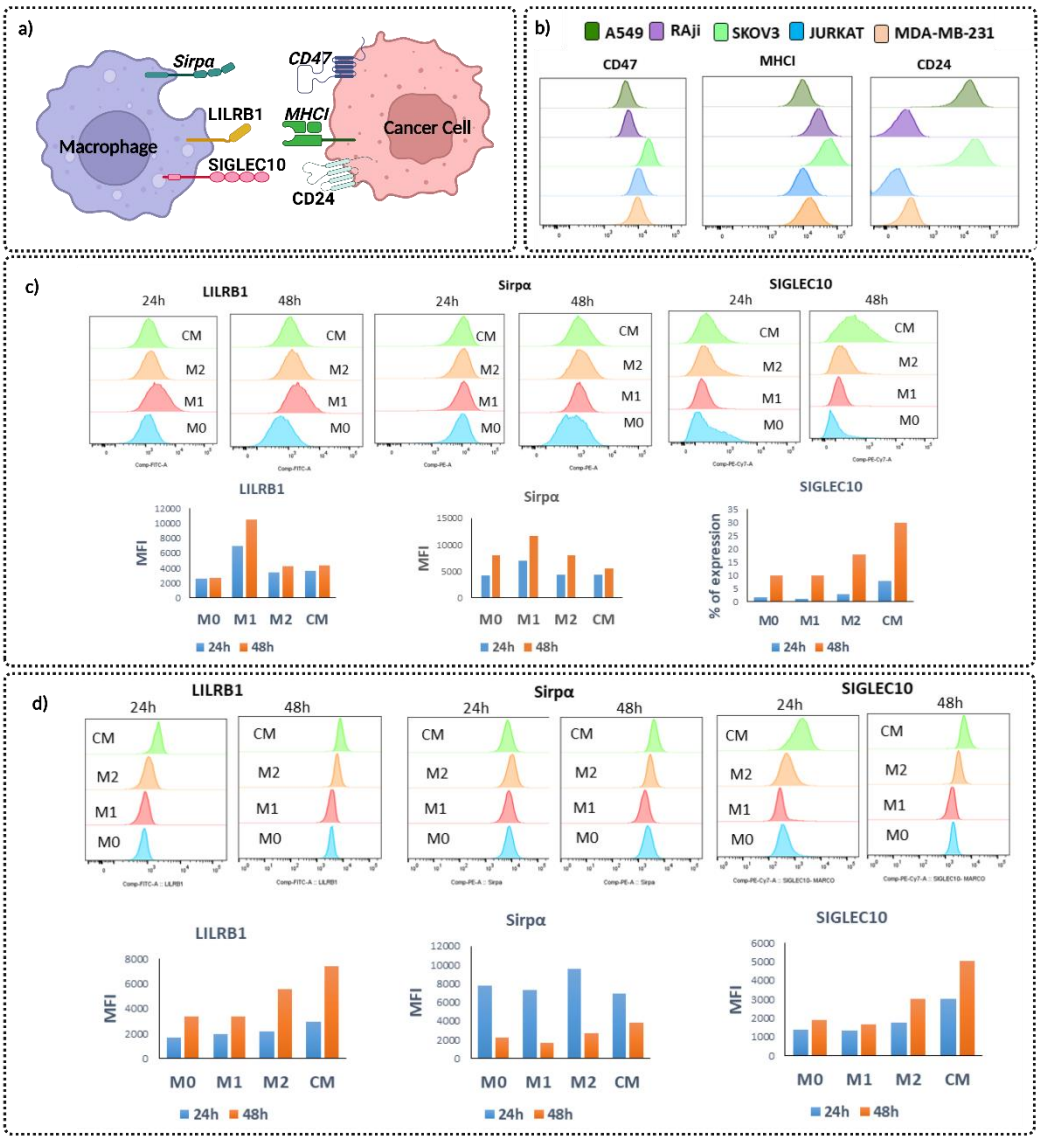

Figure 7 a) Schematic representation of the "don't eat me" signal CD47, MHCI, and CD24 and SIRPα-SIGLEC10-LILRB1 receptors respectively expressed by cancer cells and macrophages. **b)** FACS analysis of the expression of "don't eat me" signal on different types of cancer cells: A549/Raji/SKOV3/Jurkat/MDA-MB-231. SKOV3 (light green histogram) shows strong expression of all three ligands. Jurkat (blue histogram) and MDA-MB-231 (orange histogram) show moderate expression of CD47 only **c)** THP1 polarization: After 24h and 48h from the polarization showed the results at the flow cytometry of the expression of the receptors. 24 hours and 48 hours after polarization the cells were analysed by flow cytometry. For LILRB1-SIGLEC10-SIRPα- the median fluorescence intensity is observed (N=2). **d)** Polarization of primary monocytes from peripheral blood. After 24h and 48h from the polarization showed the results at the flow cytometry of the expression of the receptors. 24 hours and 48 hours after polarization the cells were analysed by flow cytometry. for LILRB1-SIGLEC10-SIRPα- the median fluorescence intensity is observed (N=2)

4.2.2 Development of SIRPα-Fc encoding synthetic circuits

After determining the expression of phagocytosis receptors, we focused on the strategies to increase the phagocytosis of cancer cells by neutralizing the "don't eat me" signals. The main disadvantage of previous strategies attempting to neutralize this axis by systemic administration of blocking antibodies is the severe toxicity due to the expression of these proteins on several cell types. For example, CD47 is highly expressed in red blood cells, and treatment with blocking antibodies causes severe forms of anaemia. The use of a SIRPα protein fused to an Fc region of human IgG1 was already reported to neutralize CD47 expressed on cancer cells effectively and to increase their phagocytosis when injected as purified protein in situ[122] . We reasoned that engineering cells for the controlled production of SIRPα-Fc would provide an effective alternative to reduce the side effects of systemic administration. Thus, we incorporated the SIRPα-Fc domain into a lentiviral vector (pHR) to generate cells where the construct would be stably integrated. I designed lentiviral vectors containing two transcriptional units (TU). The first TU includes the inducible promoter UAS responding to the transcription factor Gal4-VP64, upstream of the IL2 signal peptide, the CV1 (SIRPα domain) sequence and Fc domain of IgG1 (the tail region of an antibody that interacts with Fc receptors) to play a role in mediating phagocytosis. The fusion protein is co-expressed with the blue fluorescent protein eBFP with a P2A self-cleaving peptide to monitor protein expression. The second TU comprises a short EF1α (shEF1α) promoter and a truncated version of the low-affinity nerve growth factor receptor (delta LNGFR), devoid of the entire cytoplasmic domain, which is used as a tag of the transduced cells (**Fig.8a**). To test the production of the SIRPα-Fc protein, the plasmid was co-transfected together with a plasmid encoding the transcription factor Gal4-VP64 in human embryonic kidney cells 293T-17 (HEK293T-17). The detection of eBFP with microscopy and flow cytometry was used as a proxy for the expression of the SIRPα-Fc protein (**Fig.8b**).

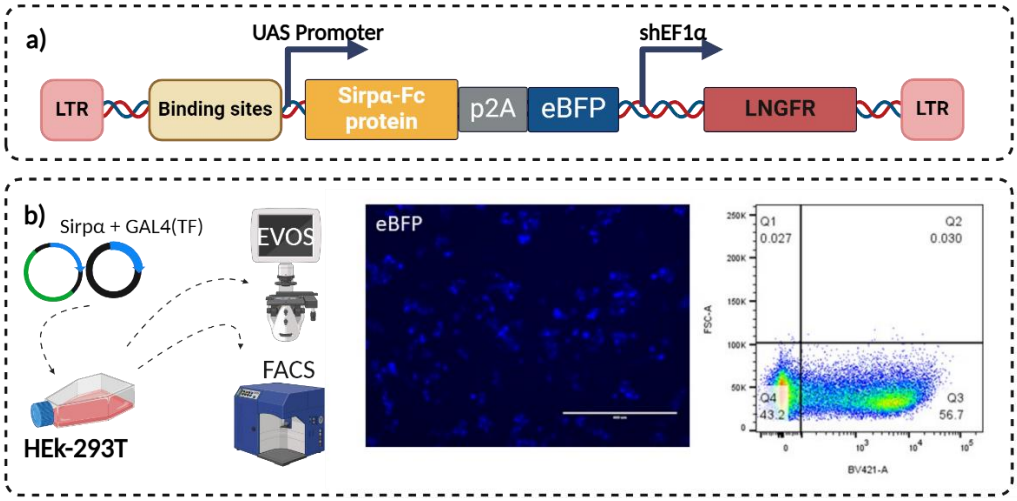

Figure 8 ***a)*** **Lentiviral vectors for cell engineering with the sensor-actuator synthetic system**. Scheme of the lentiviral vectors (LVs) that were designed to engineer cells with SIRPα-Fc protein. They include two independent transcriptional units (TU) in the same orientation. the SIRPα-Fc coding sequence was inserted in the first TU under the control of an inducible promoter (UAS), which is responsive to the GAL4 transcription factor. When co-transfected GAL4 drives the expression of Sirpα -Fc and eBFP reporter. The second TU comprises the constitutive shEF1α promoter driving the expression of a truncated version of the low-affinity nerve growth factor receptor (LNGFR) lacking the entire cytoplasmic domain that was used as a transduction marker. **b)** eBFP protein expression was assessed by microscopy and flow cytometry.

4.2.3 Competitive anti-CD47 binding assay

The binding of SIRPα-Fc secreted in the medium to CD47 was initially verified by flow cytometry-based competition assay using SKOV3, MDA-MB-231, and Jurkat cell lines that naturally express CD47. If the SIRPα-Fc protein efficiently binds the target, it prevents the binding to CD47 of a fluorophore-conjugated mAb anti-CD47, therefore reducing the emitted signal. In other terms, the SIRPα-Fc protein and the mAb compete for CD47 binding resulting in a decrease of the CD47 signal in the presence of secreted SIRPα-Fc protein. The competition assay was performed by incubating non-transfected tumor cells with SIRPα-Fc protein supernatant (SN) to mimic the conditions in which Sirpα-Fc secreted by engineered macrophages act on surrounding tumor cells. HEK293T-17 cells were co-transfected with the UAS-SIRPα-Fc plasmid and a plasmid constitutively expressing the GAL4-VP64 transcription factor (TF) to activate the system. After 48 hours, the SN was harvested and transferred to the tumor cells (**Fig. 9a**). MDA-MB-231 (**Fig.9b**), SKOV3 (**Fig.9c**), and Jurkat cells (**Fig.9d**) were treated with SN for 3 hours before staining with the anti-CD47 mAb. In all cell lines, a significant blockade of CD47 was

observed when tumor cells were treated with a supernatant of cells transfected with SIRPα–Fc protein. Overall, the competition assay results demonstrated and highlighted the capacity of SIRPα-Fc protein to bind CD47.

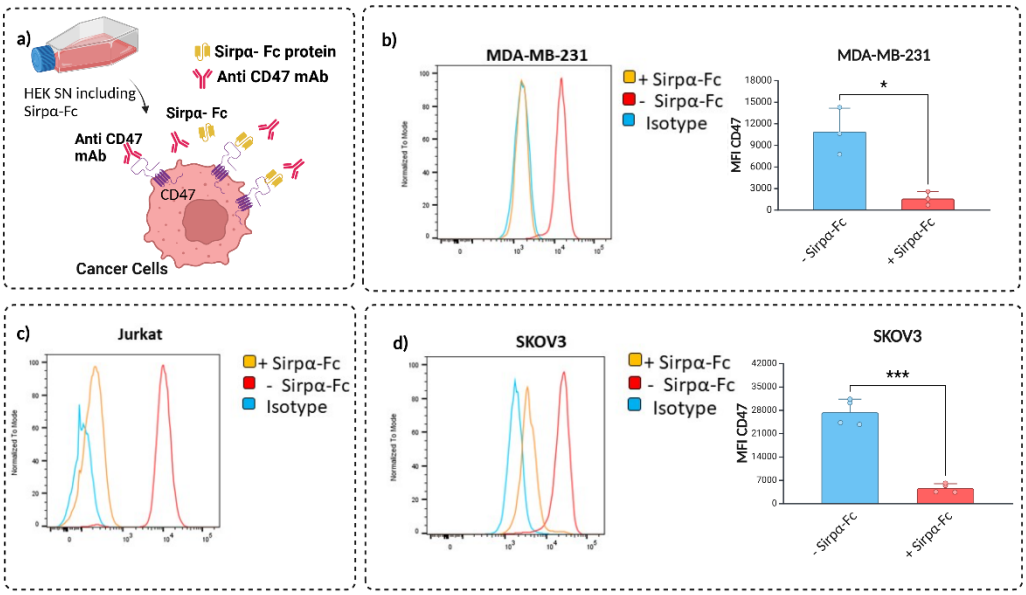

Figure 9 Competitive binding assay. ***a)*** Schematics of the assay*:* MDA-MB-231, SKOV3, and Jurkat cells were treated with supernatant (SN) of HEK293T-17 cells 48h post-transfection with GAL4- VP64 TF and SIRPα-Fc. **b-c-d)** MDA-MB-231, SKOV3, and Jurkat cells were treated with SN from the transfection for 3 hours and then stained with anti-CD47 mAb. The presence of SIRPα protein reduces CD47-antibody signal (orange histogram) when compared with signal of the conjugated antibody alone (red histogram), indicating the competition for the binding to the CD47. SIRPα-Fc control indicated the basal CD47 expression. **b-d*)*** The bar plot shows the mean ± standard error of the mean (SEM). The statistical test is a two-tailed paired t-test (* = p-value < 0.05 (N=3); *** = p-value < 0.001 (N=4))

4.2.4 Phagocytosis Assay with THP-1

After confirming the presence of the SIRPα-Fc protein in the supernatant of transfected HEK-293T cells, the next step was to assess its efficacy in increasing phagocytosis. Specifically, I tested the phagocytosis of Jurkat cells in co-culture with macrophages polarized into the three different phenotypes (M0, M1, M2). We hypothesized that in the presence of SIRPα-Fc, we would observe an increase in Jurkat cells engulfed through flow cytometry. Following the polarization protocol described in **Fig.6a**, FITC-labeled Jurkat cells were incubated for 3 hours with macrophages 24 hours from the beginning of the polarization. The same procedure was repeated after 48 hours of polarization. During these co-culture experiments, the

supernatant from HEK-293T cells that contain SIRPα-Fc protein was added to the system, and flow cytometry was used to compute the percentage of engulfed cells (**Fig.10a**). To distinguish macrophages from Jurkat cells, the formers were stained with the monoclonal antibody (mAb) CD11b. For the analysis, we selected the double-positive population for FITC (Jurkat) and CD11b (macrophages) and then calculated the percentage of green-labelled Jurkat cells that had been engulfed within this double-positive population. The results demonstrated a significant increase of phagocytosis in the presence of SIRPα-Fc across all three macrophage phenotypes (M0, M1, M2) (**Fig.10b**). These preliminary findings indicate that SIRPα-Fc, binding to CD47 on tumor cells, enhances phagocytosis by polarized macrophages and represents a promising tool for boosting macrophage-mediated tumor cell clearance.

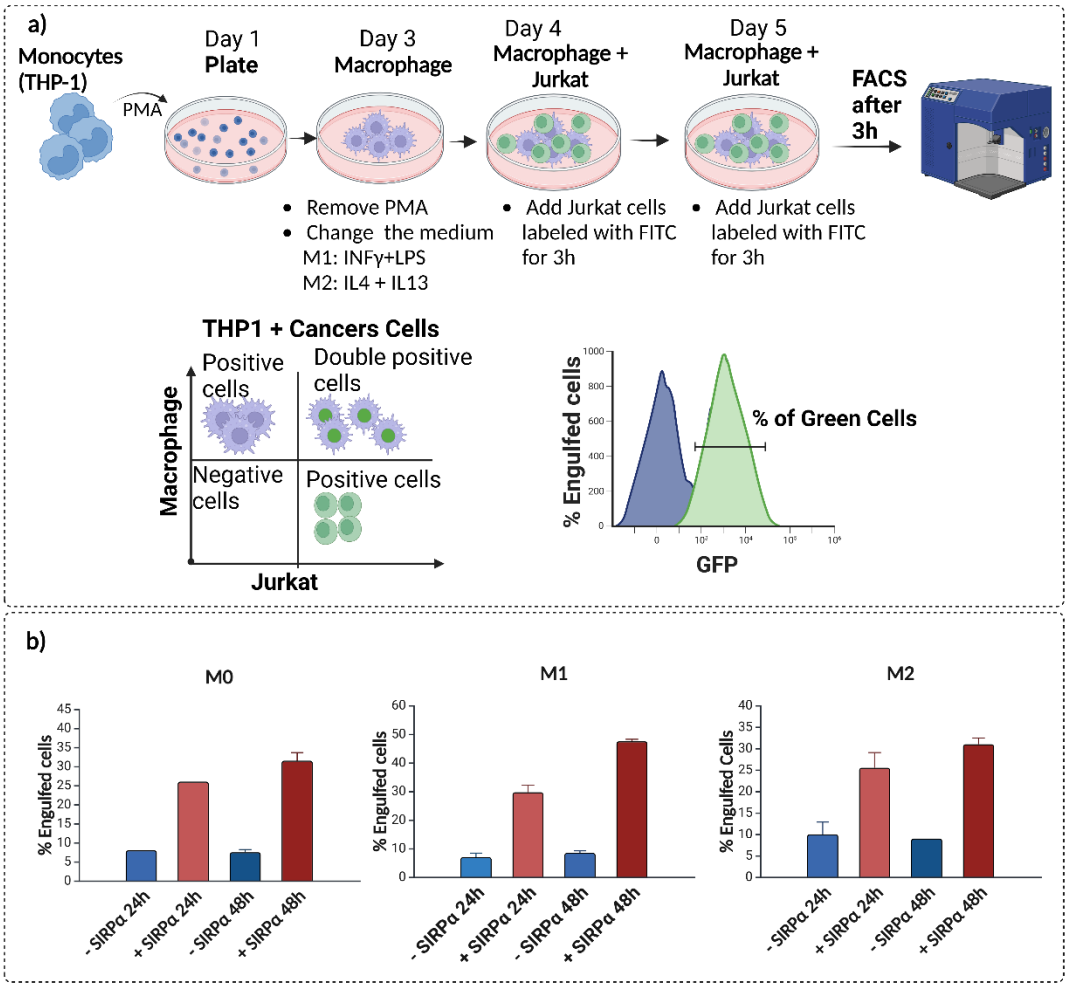

Figure 10 a) Schematic representation of the experimental workflow of phagocytosis following THP-1 polarization. The polarization of THP1 is performed by adding PMA to the plate for 48h followed by specific cytokine treatment to induce phenotypes M1 or M2. After 24h

and 48h from the polarization Jurkat cells marked with CSFE FITC were added to the culture for 3h in the presence or absence of supernatant (SN) with SIRPα-Fc protein. After 3h cells were detached and stained with CD11b mAb to analyse the engulfed cells by flow cytometry (double positive population indicate engulfed macrophages). **b) percentage of phagocyted cells**. In M0-M1-M2 an increase in phagocytosis can be observed in the presence of the SIRPα-Fc protein compared to control (CTRL) without SIRPα-Fc protein, which is further enhanced 48h of post-polarization of THP1. (N=2)

4.2.5 THP-1 Cell Engineering with sensor-actuator synthetic system

4.2.5.1 Stable integration of sensor-actuator in the THP1 cell line

The results of the various tests above indicate that the SIRPα-Fc protein recognize the CD47 target, disrupt the SIRPα-CD47 interaction, and enhance the phagocytosis of tumor cells in an in vitro model. To achieve the primary objective of arming macrophages with genetic circuits composed of a sensor module and an actuator module, we incorporated this sensor/actuator construct into a lentiviral vector. The sensor modules are represented by SynNotch receptors developed in the group, while the actuator module consist of the SIRPα-Fc protein. SynNotch was chosen because it leverages the Notch signaling pathway by utilizing the transmembrane domain of native Notch receptors, with an extracellular domain that can be customized and an internal domain acting as transcription factor (TF). Coupling cellular sensing with a given response would be highly beneficial for engineering therapeutic cells. THP-1 cell lines that stably express the complete sensor/actuator circuit were generated through transduction with second-generation lentiviral vectors. I co-transduced the cells using a lentiviral vector encoding SynNotch marked with a Myc tag (details cannot be disclosed as they are under patent application) along with the lentiviral vector encoding SIRPα-Fc, as described in section 4.2.2. Seven days post-transduction, extracellular staining with an anti-LNGFR monoclonal antibody (present in the SIRPα construct) and an anti-Myc tag antibody (present in the extracellular domain of SynNotch) was performed to evaluate transduction efficiency. The results showed balanced expression levels for both markers, with approximately 50% of the cells positive for either LNGFR or Myc. Given that the percentage of double-positive cells (co-expressing both lentiviral vectors) was around 26%, we performed a sorting for both markers, yielding a pure population with 90% double-positive cells (**Fig.11**)

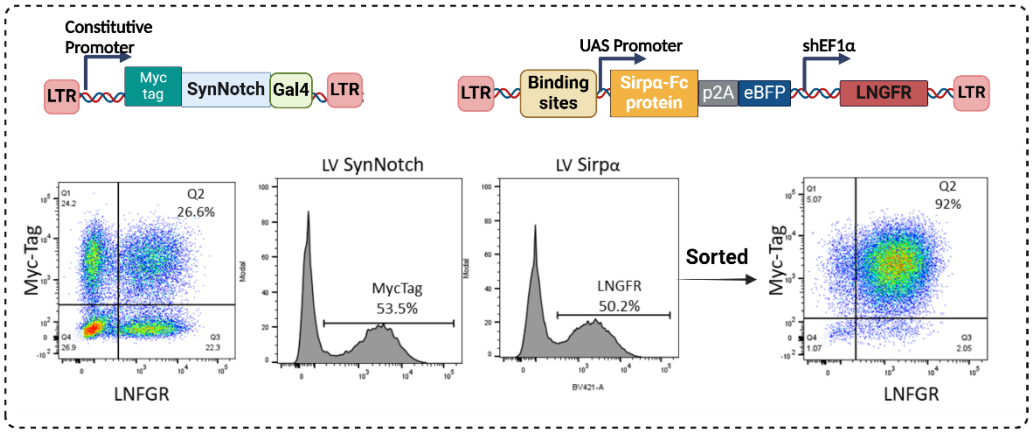

Figure 11 Lentiviral vectors for engineering THP1 with the sensor-SIRPα-Fc synthetic system. A Lentiviral vector (LV) was designed to establish a stable THP1 cell line that expresses the synthetic SynNotch receptor (sensor) and the inducible SIRPα-Fc protein (actuator). The LV encoding SIRPα-Fc consists of two independent transcription units (TU) in tandem. The coding sequence for SIRPα-Fc is inserted into the first TU, under the control of an inducible promoter (UAS), which is activated when the SynNotch receptor recognizes its specific ligand, leading to the expression of SIRPα-Fc via the GAL4-VP16 transcription factor. This TU also includes a P2A self-cleaving peptide linked to the eBFP fluorescent protein, allowing for detection of system activation. The second TU is driven by the constitutive promoter shEF1α, which directs the expression of the truncated LNGFR, serving as a transduction marker. The SynNotch coding sequence is under the control of a constitutive promoter, and the MycTag protein is used as a transduction marker. Initially, a mixed cell population was created, with 26% of the cells being positive for both MycTag and LNGFR. This population was subsequently sorted to achieve a purified population with 90% positivity.

4.2.5.2 Activation of the system sensor-actuator in the presence of specific ligand

Following the creation of engineered macrophages with the sensor/actuator circuit (also called the "receiver" line), the strategy for developing sensor modules involved engineering "sender" cell lines. In the lab, a Jurkat cell line was created both with and without the ligand specific for the SynNotch sensor. When our receiver cell line is co-cultured with Jurkat cells lacking the ligand, no expression of the eBFP protein is expected, indicating no system activation. However, when co-cultured with Jurkat cells expressing the ligand, eBFP protein expression in the receiver cells should indicate system activation (**Fig.12a**). We performed a co-culture in suspension of the receiver cell line with the sender line both in absence or presence of the ligand. After 48 hours, we analyzed the cells via flow cytometry to detect eBFP protein expression. The BFP reporter was expressed by roughly 20% -30% of the total receiver population **(Fig.12b)**, demonstrating that our sensor/actuator system can be activated by the target. To further assess functionality, we performed a CD47 competition assay. Instead of using the supernatant produced by HEK-293T cells, as

described in section 4.2.3, we carried out the assay directly on the Jurkat cells used in the co-culture with the receiver THP1. In the presence of the ligand that activates the circuit, decreased CD47 signal (green histogram) was observed, as compared to the basal CD47 level and to the circuit without the ligand (red and orange histograms) (**Fig.12c**). This result suggests that upon circuit activation the SIRPα-Fc protein is being released and binds to CD47 on tumor cells.

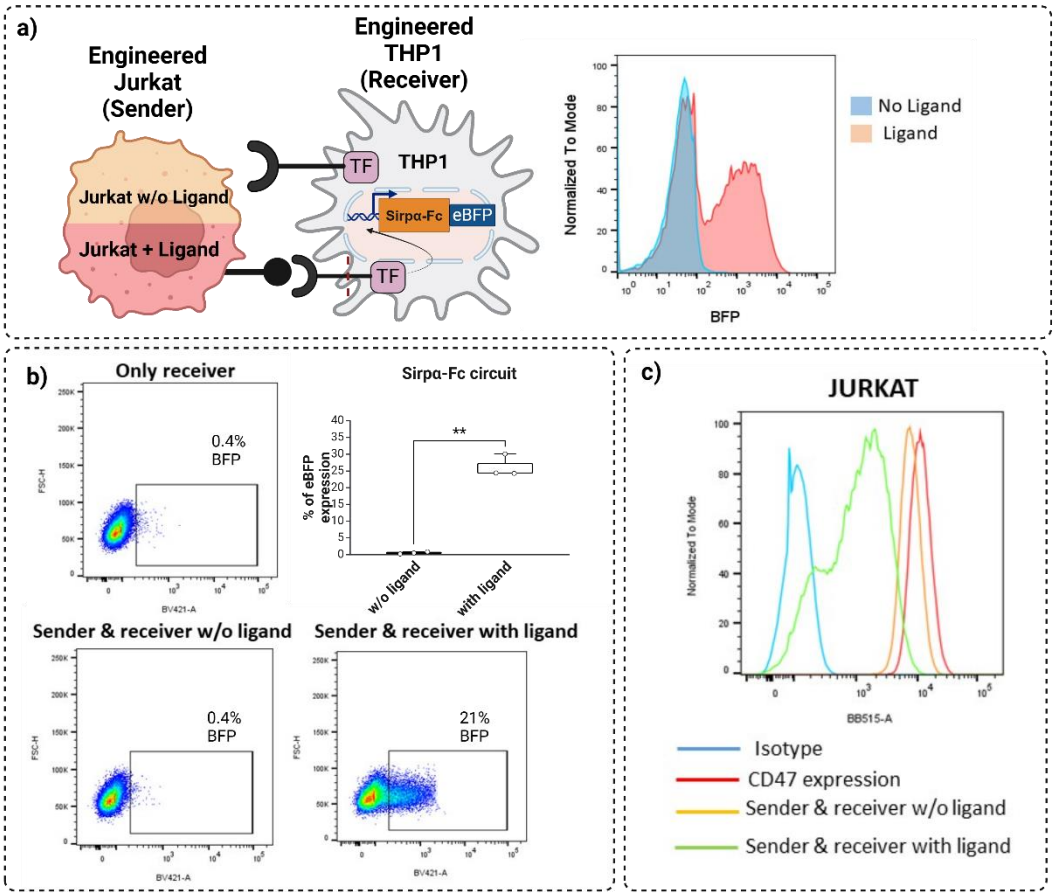

Figure 12 a) Schematic representation of the complete sensor/actuator circuit. In the presence of Jurkat wt (no ligand), the synthetic receptor is not activated and no expression of the eBFP protein should be observed. Jurkat expressing the ligand should instead trigger eBFP expression by interaction with the SynNotch. **b) BFP expression in the receiver cells**. The fraction of cells expressing eBFP is plotted from co-culture in suspension of THP-1 receiver cells with Jurkat wt and with Jurkat expressing the SynNotch ligand (treated). Each dot represents a biological replicate for each independent experiment (N=3), while the bar plot shows the average of the means ± standard error of the mean (SEM). The statistical test used is a two-tailed paired t-test (** = p-value < 0.005). **c) Competition assay on Jurkat cells.** The presence of SIRPα protein secreted by activated circuit reduces the CD47-antibody signal (green histogram) when compared with the basal expression (red histogram) and with the system not activated (orange histogram), indicating the competition for the binding of the antibody to the CD47.

4.2.5.3 Sensor-Actuator system: release of SIRPα-Fc protein

The next step was to validate the functionality of the circuit by examining the phagocytosis mechanism via flow cytometry (as described in paragraph 4.2.4). To do this, we transitioned the co-culture of sender/receiver cells from suspension to adhesion. We plated the receiver cells in the presence of PMA, and after 48 hours, we detached them and co-cultured them with Jurkat cells (labeled with CFSE-FITC) in the presence and absence of the ligand. At the same time, we added a cytokine cocktail at co-culture to induce differentiation and re-plated the cells (since the THP1 cells had matured into macrophages after 48 hours of PMA treatment, they naturally re-adhered to the plate). 48 hours post co-culture, we analyzed the percentage of phagocytosed cells using flow cytometry (**Fig.13**)

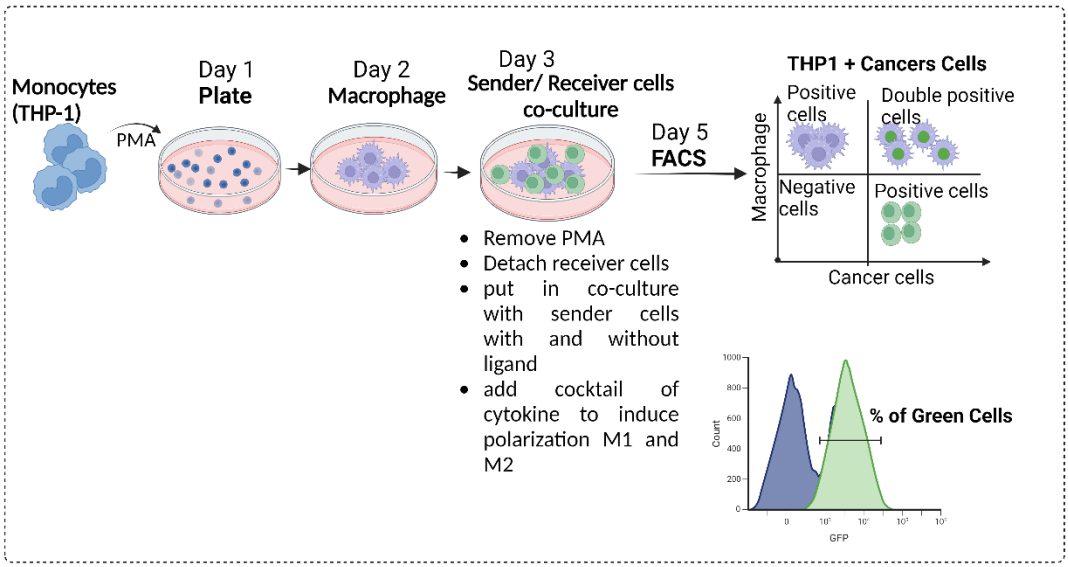

Figure 13 Schematic representation of circuit sensor/actuator in adhesion. The polarization of THP1 is performed by adding PMA to the plate. After 48h the PMA is removed, the mature macrophages are detached and placed in co-culture with Jurkat with or without the ligand marked with CFSE FITC membrane dye. The macrophages/jurkat are seeded in the plate, and at the same time polarization to M1 and M2 is induced. 48h post polarization we marked Macrophage with CD11b mAb and we analyzed the engulfed cells at FACS (double positive population)**.**

The results showed that eBFP is expressed in the presence of the ligand, particularly in the M2 phenotype. In adhesion, an increase in the leakiness of the SynNotch system was observed, though it was still lower than the expression in the ligand-activated system. In fact, the difference in eBFP activation was significant also in adhesion **(Fig.14a**). When analysing the engulfed cells, a modest but significant increase in phagocytosis was observed between the activated and non-activated

systems in all phenotypes. Notably, the increment in phagocytosis upon circuit activation was higher in the M2 phenotype if compared to the M1 phenotype (**Fig. 14b**). This result may be advantageous as the M2 phenotype has well established pro-tumorigenic functions. All these results further support the efficacy of the sensor/actuator model, showing a positive response in increasing phagocytosis and suggesting potential applications of this platform in cell-based therapy.

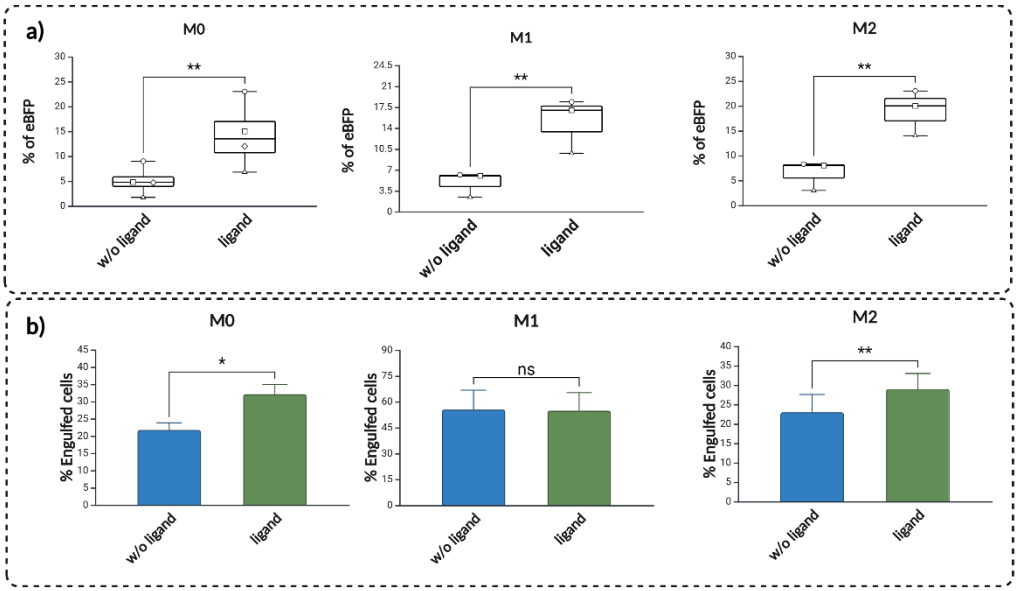

Figure 14 Activation of sensor/actuator circuit in adhesion. a) eBFP reporter expression. The fraction of cells expressing BFP is plotted from co-culture in adhesion of THP-1 receiver cells polarized in different phenotype with Jurkat wt and with Jurkat expressing the synNotch ligand. Each dot represents an independent experiment (N=3), while the bar plot shows the mean of the means ± standard error of the mean (SEM). The statistical test used is a two-tailed paired t-test (** = p-value < 0.05). **b)** Bar plot of the % of engulfed cells from co-culture of THP-1 receiver cells polarized in different phenotype with Jurkat wt and with Jurkat expressing the synNotch ligand. Each dot represents an independent experiment (N=3), while the bar plot shows the mean of the means ± standard error of the mean (SEM). The statistical test used is a two-tailed paired t-test. M0(* = p-value < 0.05) M1(p-value=ns) M2(**=p-value<0.005).

4.3 Characterization of therapeutic actuator 2

4.3.1 Development of Bacterial Compound synthetic circuit

The second actuator that we developed has the scope to repolarize the TAMs from the M2 to M1 phenotype. Bacterial components, such as lipopolysaccharides (LPS) or other pathogen-associated molecular patterns (PAMPs), can stimulate macrophage receptors like Toll-like receptors (TLRs), inducing an inflammatory response. The use of bacterial components represents a form of immunotherapy that leverages the immune system to target diseases rather than directly attacking pathogens or malignant cells. These components can be strategically directed to activate an M1 response only in areas of need, such as tumor sites or infections, potentially minimizing side effects. To achieve this, we created an alternative version of the lentiviral construct SIRPα-Fc, replacing the Fc domain with a [redacted] (BC) (**Fig.15a**), which was previously shown to induce repolarization of TAMs *in vivo* when secreted by a different bacterial species[122].The lentiviral plasmid is constructed as for the first actuator described in Chapter 4.2.2. The concept of utilizing the BC protein is to harness a dual effect. The hypothesis is that through the release of SIRPα binding to CD47, preferential binding to cancer cells occurs, while simultaneously activating macrophage repolarization through the action of BC. As for the previous actuator, the production of the protein BC could be induced by co-transfection with a plasmid encoding for the transcription factor Gal4-VP64 in HEK293T-17. Expression of the BFP reporter can be used as a proxy for the production of the BC protein (**Fig.15b**).

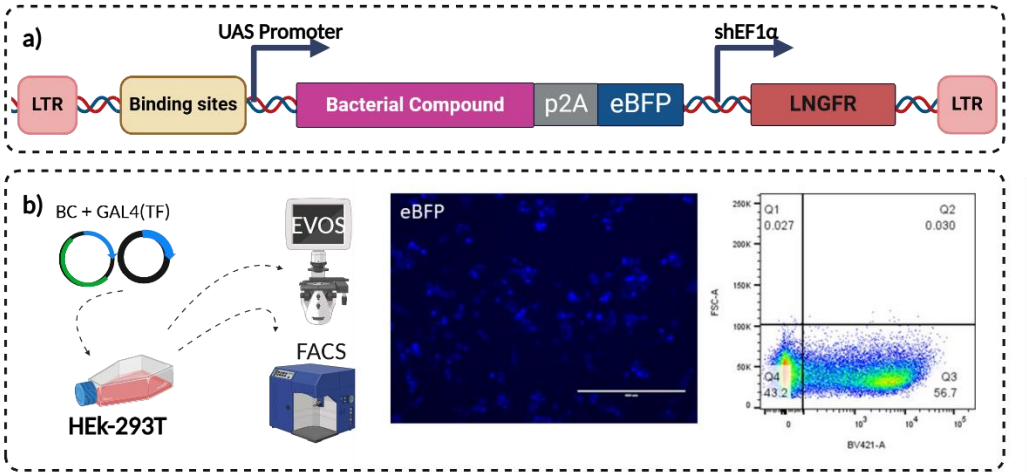

Figure 15 a) Lentiviral vector for engineering THP1 with the sensor-BC synthetic system. Scheme of the lentiviral vector (LV) that was designed to engineer cells with BC-based actuator. They include two independent transcriptional units (TU) in tandem. BC coding sequence was inserted in the first TU under the control of an inducible promoter (UAS), which is responsive to the GAL4-VP16 transcription factor. When co-transfected GAL4-VP16 TF drives the expression of BC and eBFP reporter. The second TU comprises the constitutive shEF1α promoter driving the expression of a truncated version of the low-affinity nerve growth factor receptor (LNGFR) lacking the entire cytoplasmic domain that was used as a transduction marker. **b)** eBFP protein expression was assessed by microscopy and flow cytometry

4.3.2 Functional characterization of Bacterial Compound protein

After the creation of the new plasmid with the BC protein, we performed functional tests by flow cytometry and ELISA to test the cellular repolarization of our model systems. After the differentiation of monocytes (THP-1 and primary monocyte) in macrophages, we carried out a protocol of re-polarization. HEK293T-17 cells were co-transfected with the inducible BC plasmid and the vector encoding the Gal4-VP64 to activate the system. 48 hours after transfection, the SN was harvested (**Fig.16a**). In the THP-1 model at day 1 plate the cells, at day 3 we added the cocktail of cytokines to induce polarization in the SN containing the BC protein and in the control without BC. In the primary monocyte model, on day 7, we induced polarization as described in **Fig. 6b** and on day 8 we added the SN with BC protein. As readout of the effects of BC on the polarization, we measured the expression of classical M1 (CD80) and M2 (CD206) markers by flow cytometry. Moreover, we performed ELISA assays to measure the expression of TNFα (tumor necrosis factor) and IL6, generally associated with inflammatory conditions, collecting the supernatant from the THP1 and primary macrophages re-polarization experiment (**Fig.16b**).

We hypothesized that, if the BC protein is bound by the TLRs, the consequence is a skewing from the M2 phenotype to M1 with pro-inflammatory cytokine release.

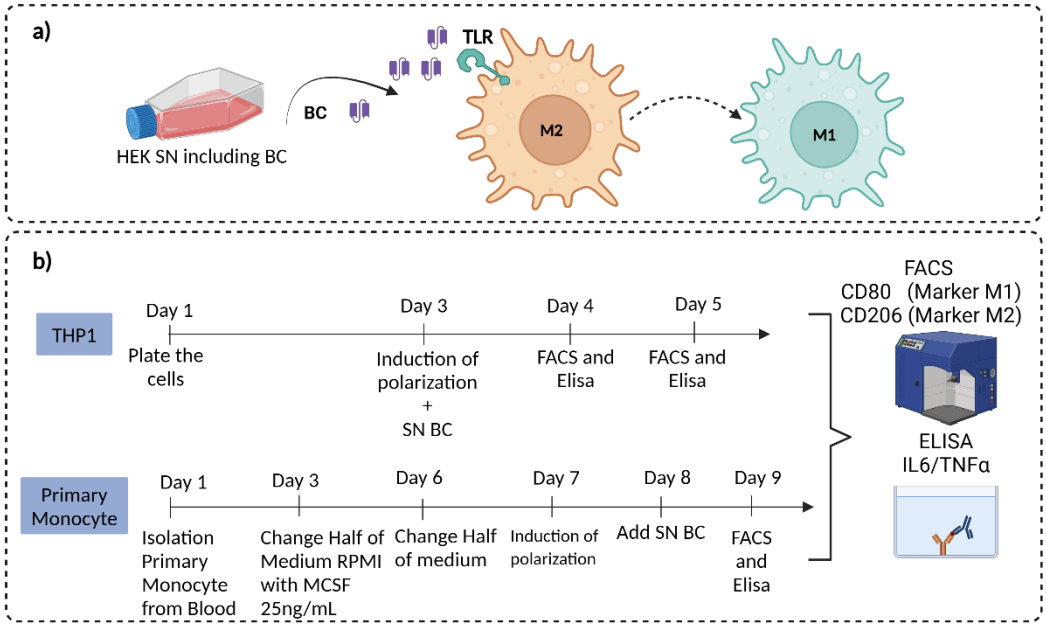

Figure 16 a) Schematic representation of BC production. Media was harvested by co-transfected HEK293T-17 cells with GAL4-VP16 TF and UAS-BC, after 48h. **b) schematic of THP1 polarization**. Maturation to macrophages is achieved by adding PMA. After 48h the PMA is removed, and polarization is induced in M1 and M2 phenotypes using medium with and without BC. After 24h and 48h from the polarization cells were analysed by flow cytometry. Medium instead was kept carrying out ELISA assays. Primary Monocyte polarization: isolation of PBMCs from buffy coats of blood donors through a density gradient centrifugation. CD14+ are isolated via negative selection and seeded with the Macrophage colony stimulating factor (M-CSF). Medium was changed every 3 days until 7 days when a complete maturation of macrophages at the state M0 is obtained. Next, a cytokine cocktail for the formation of the phenotype M1 and M2 is added. At day 8, we added the media with and without BC. After 48h of polarization we analysed the result by flow cytometry and collected the media for ELISA.

4.3.2.1 Re-polarization of THP-1 cells

Following the protocol described in **Figure 16b**, we analyzed the expression of CD206 marker via flow cytometry 24 and 48h post-polarization.

The results showed a reduction in CD206 associated signal in the M2 phenotype polarized in the presence of BC compared to standard polarization, both 24 and 48 hours after the cytokine administration (**Fig.17a**). To confirm the presence of BC in our system, we performed the same polarization experiment as shown in **Figure 16b** on a cell line called THP1- a modified THP1 cell line designed to detect the interaction between Toll-like receptor (TLR) and BC. If the TLR-BC binding occurs, the inflammatory cascade activates the NF-κB transcription factor, which induces the expression of a reporter gene SEAP (secreted embryonic alkaline phosphatase) (**Fig.17b**). Therefore, we induced the polarization of the THP1- line assessing the expression of the SEAP reporter in the presence of the BC in the SN. Additionally, we measured the release of pro-inflammatory cytokines using ELISA. We performed SEAP and ELISA assays on the supernatant collected from these polarization experiments. The results showed that SEAP was expressed when the THP1 were cultured with medium containing the BC protein, compared to cells cultured without BC (**Fig.17c**). To test these findings in an alternative way, we performed ELISA assays to detect the induction of TNF-α and IL-6 production by BC. In the M1 phenotype, high levels of both cytokines could be found confirming the acquisition of a pro-inflammatory phenotype. More importantly, we detected increased expression of TNF-α and IL-6 in the M2 phenotype in the presence of BC if compare with the basal level (**Fig. 17d**). These results suggest an ongoing repolarization from the M2 to the M1 phenotype.

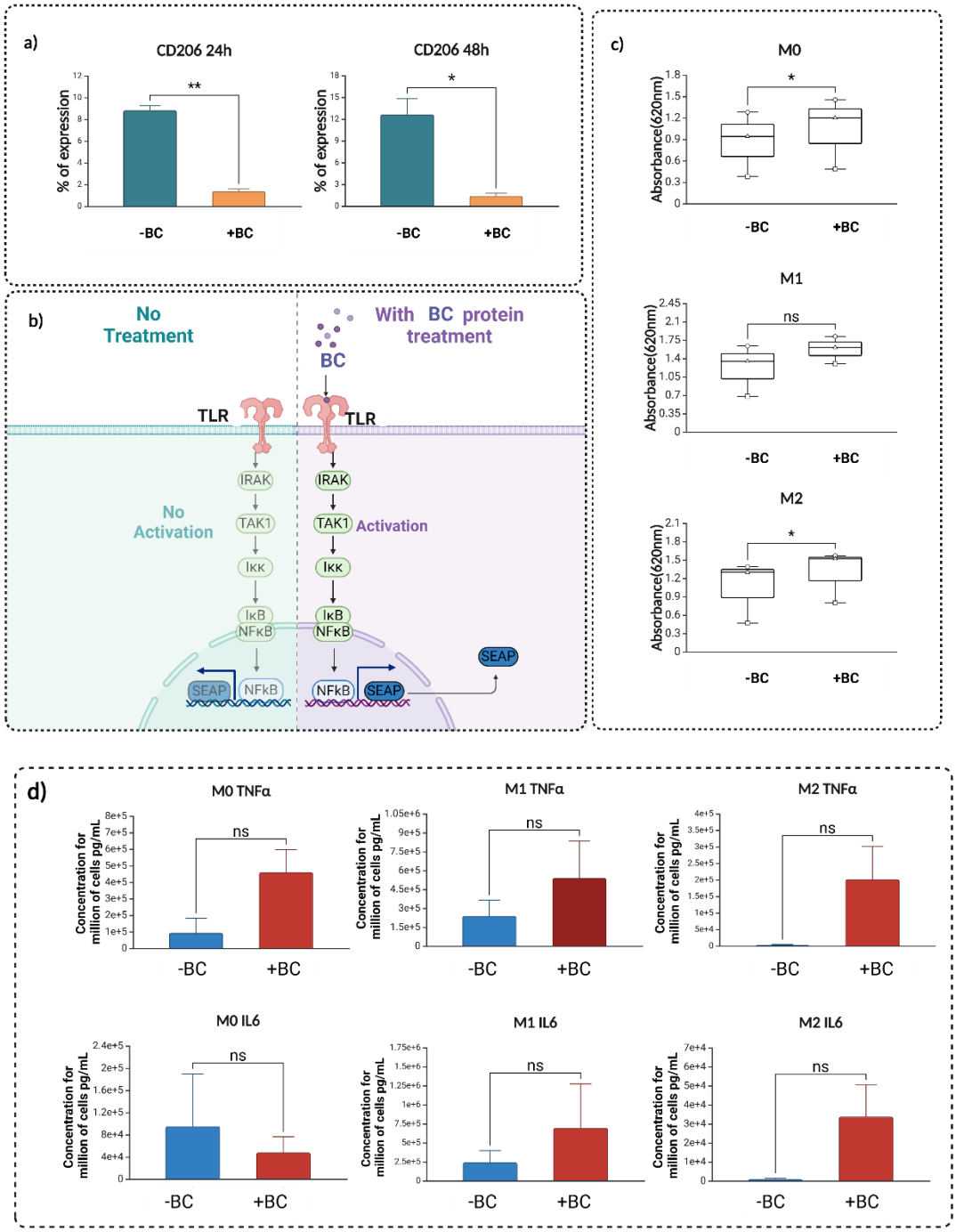

Figure 17 a) % of cells expressing CD206, a M2 marker. CD206 expression decreases in the presence of BC protein if compare with the control without BC. Each dot represents an independent experiment (N=3), while the bar plot shows the average of the means ± standard error (SEM). The statistical test used is a two-tailed paired t-test CD206 24h (** = p-value < 0.005) CD206 48h (* = p-value <0.05. **b) Graphical representation of the SEAP test using [redacted] THP1 cells**. In the absence of BC, the inflammatory pathway is not activated. In the presence of the BC that recognize TLR, there is activation of the inflammatory cascade NFkβ binds its binding domain with subsequent production of the SEAP protein. **c) SEAP assay.** Level of Optical Density at 620nm (due to the presence of SEAP reporter protein) measured in the supernatants with In-Spire instrument. The optical density has been detected at 3h of incubation. The supernatants were derived from colture of 48h of THP-1 [redacted] polarized in M0-M1-M2 in the presence and absence of BC. The results show an increase of SEAP protein in the presence

of BC. Each dot represents a biological replicate (N=3), while the bar plot shows the mean of the average ± standard error (SEM). The statistical test used is a two-tailed paired t-test M0 (* = p-value < 0.05) M1 (ns) M2 (* =p-value <0.05) **d) ELISA assay.** The level of luminescence (concentration pg/mL) is normalized on number for millions of cells. The supernatants were derived from colture of 48h of THP-1 [redacted] polarized in M0-M1-M2 in the presence and absence of BC. The results show that in the presence of BC in M2 phenotype (anti-inflammatory) the production of inflammatory cytokines IL6 and TNFα increases (N=3). The bar plot shows the average of the means ± standard error of the mean (SEM). The statistical test used is a two-tailed paired t-test M0-M1-M2 (ns).

4.3.2.2 Re-polarization of CD14+ cells

To understand whether the addition of BC induces a repolarization from phenotype M2 to M1 in the primary macrophages, I analysed the expression of the markers CD80 (M1) and CD206 (M2). The results show that in the presence of BC after 48h of polarization as described in Figure 16b, the expression of CD80 increases in the phenotype M0 and M2 (blue and orange histograms). CD206 expression in the phenotype M2 (orange histogram) in the presence of BC is strongly reduced and becomes similar to M1 and M0 (red pick and blue histograms) **(Fig.18a).** Interestingly, preliminary data of the ELISA assay with the medium collected from the repolarization experiment described above indicate increased production of TNFα and IL6 (pro-inflammatory cytokines) across all phenotypes. In specific, in M1 condition, this confirms the correct polarization, whereas in M2 this suggest a potential skewing of the polarization (**Fig.18b**). These preliminary results suggest that the BC protein recognizes its TLR receptor which activates the NFk-β signal cascade with subsequent release of pro-inflammatory cytokines that makes the environment prone to a repolarization from phenotype M2 to phenotype M1.

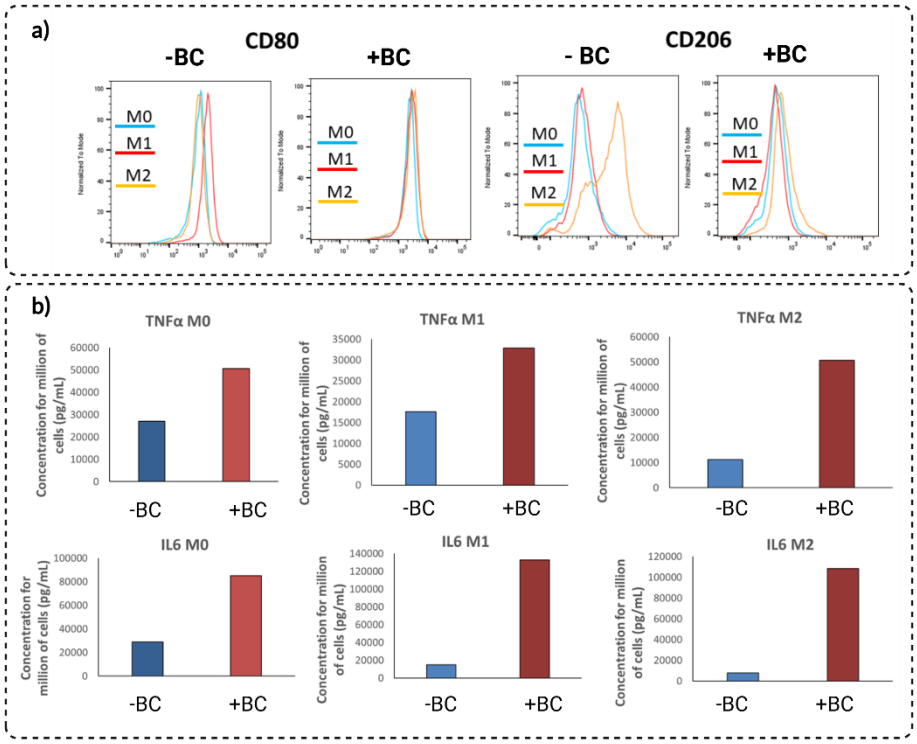

Figure 18 a) Flow cytometry analysis of cells after 48h to assess polarization in the presence or absence of BC. In the absence of BC, the M1 marker CD80 is expressed (red histogram). With BC, CD80 expression increases in M0 (blue histogram) and M2 (orange histogram) overlapping with M1. The M2 marker CD206 is highly expressed in the absence of BC (orange histogram) but not in M0 (blue histogram) or M1 (red histogram). BC addition significantly reduces CD206 in M2, aligning it with M0 and M1 levels. (N=2). **b) ELISA assay.** The level of Luminescence (concentration pg/mL) is normalized on number for millions of cells. The supernatants were derived from culture of 48h of primary monocyte cells polarized in M0-M1-M2 in the presence and absence of BC. Preliminary data show that in the presence of BC in M2 phenotype (anti-inflammatory) there is production of inflammatory cytokines IL6 and TNFα.

5 Conclusion

In recent decades, cancer therapy has made significant strides, particularly with the advent of immunotherapy, which harnesses the patient's immune system to target and destroy tumor cells. One of the most promising advancements in this field is CAR-T cell therapy. However, its effectiveness against solid tumors is hindered at least in part by the immunosuppressive nature of the tumor microenvironment (TME), which creates barriers that prevent immune cell infiltration and suppress T cell activity. An alternative approach is the use of engineered macrophages, which offer several advantages in targeting solid tumors. Unlike T cells, macrophages are naturally inclined to infiltrate tumors, as they are a key part of the TME. Through synthetic biology, macrophages can be reprogrammed to perform potent anti-tumor functions once they reach the TME. In this study, a synthetic biology approach was proposed to create engineered macrophage cells as a means of rewiring the TME to promote immune response against cancer cells. Specifically, a synthetic system was created for macrophage engineering by combining a biosensor, represented by synthetic receptors responsive to specific ligands present in the TME, with two types of actuators aiming at i) enhancing phagocytic activity of macrophages and ii) skewing macrophage polarization towards an M1 phenotype.

CD47-targeting therapies have emerged as promising tools in cancer immunotherapy by blocking the "don't eat me" signal used by tumor cells to evade immune destruction. While effective at enhancing macrophage-mediated phagocytosis of tumor cells, CD47-targeting antibodies have faced significant challenges due to the high expression of CD47 on various healthy cells, especially red blood cells (RBCs). This broad expression can lead to off-target effects, such as anemia from unintended RBC phagocytosis, and can also cause immune-related toxicities like neutropenia and thrombocytopenia. Addressing these issues requires a more selective approach that confines CD47-targeting activity to the tumor microenvironment (TME) and minimizes exposure to healthy cells. In recent studies, including the work of Evangelos Stefanidis et al[116], CAR-T cells were engineered to secrete a high-affinity CV1 (SIRPα variant) as a decoy to block CD47 and enhance tumor phagocytosis. While this approach successfully boosted anti-tumor activity, it also introduced critical limitations due to its paracrine mechanism of action. In fact,

SIRPα inadvertently bound to the CAR-T cells themselves, marking them for phagocytosis by macrophages and leading to significant depletion of the therapeutic T cells. Even when the decoy expression was inducible rather than constitutive, the high affinity of SIRPα-Fc for CD47 still caused unintended phagocytosis of CAR-T cells, underscoring the risks associated with high-affinity decoy proteins in an uncontrolled release system. To overcome these challenges, we developed an alternative approach by engineering macrophages themselves to express the CD47-targeting actuator, specifically SIRPα variant (CV1) fused to an Fc region, but under the control of a synthetic Notch (SynNotch) sensor system. This configuration enables the release of the SIRPα-Fc protein only within the TME, where the SynNotch receptor is activated by TME-specific ligands. This targeted activation limits CD47 blockade activity to tumor sites, reducing the risk of adverse effects on healthy cells and preventing the unintended clearance of therapeutic immune cells, an issue seen in the CV1 CAR-T cell model. Our results demonstrated that the sensor-actuator model effectively enhanced phagocytosis of tumor cells by macrophages in the TME. Importantly, we observed a marked increase in phagocytosis when the system was activated, with M2-polarized macrophages benefiting in particular of the boost in phagocytosis promoted by the SIRPα-Fc protein. Since M2 macrophages are commonly found within the TME and often aid in tumor progression, reprogramming these cells to target tumor cells directly represents a significant therapeutic advantage. The selective action of the SIRPα-Fc actuator avoids the pitfalls of systemic CD47-targeting approaches, which can lead to broad immune suppression and depletion of healthy cells. By controlling the release of SIRPα-Fc exclusively in the TME, this engineered macrophage system offers a safer and more targeted alternative to traditional CD47-targeting antibodies and CAR-T cell models using SIRPα-Fc. This localized control aligns with the growing need in immunotherapy for precise, condition-specific activation of immune modulators, which can minimize systemic toxicities and enhance efficacy within the tumor. Additionally, the selective targeting of the TME enables this model to serve as a supportive platform for combination therapies, potentially boosting the effectiveness of CAR-T cell or other immune therapies without the risk of therapeutic cell depletion seen in the SIRPα-Fc model.

Future in *vivo* studies will be critical for assessing the therapeutic potential and safety profile of this approach in a clinical setting. In addition to boosting phagocytosis—which primarily targets macrophages within the tumor microenvironment (TME)—an equally impactful therapeutic approach lies in reversing immunosuppression to activate a robust immune response directed against cancer cells. [redacted]

[redacted]

6 References

1. Cameron, D. E., Bashor, C. J. & Collins, J. J. A brief history of synthetic biology. *Nat Rev Microbiol* **12**, 381–390 (2014).
2. Andrianantoandro, E., Basu, S., Karig, D. K. & Weiss, R. Synthetic biology: New engineering rules for an emerging discipline. *Mol Syst Biol* **2**, 1–14 (2006).
3. Bower, A. G., McClintock, M. K. & Fong, S. S. Synthetic biology: A foundation for multi-scale molecular biology. *Bioeng Bugs* **1**, 309–312 (2010).
4. Chao, R., Yuan, Y. & Zhao, H. Recent advances in DNA assembly technologies. *FEMS Yeast Res* **15**, 1–9 (2015).
5. Hutchison, C. A. *et al.* Design and synthesis of a minimal bacterial genome. *Science (1979)* **351**, (2016).
6. Zhao, N. *et al.* Synthetic biology-inspired cell engineering in diagnosis, treatment, and drug development. *Signal Transduct Target Ther* **8**, (2023).
7. Purnick, P. E. M. & Weiss, R. The second wave of synthetic biology: From modules to systems. *Nat Rev Mol Cell Biol* **10**, 410–422 (2009).
8. Menolascina, F., Siciliano, V. & Di Bernardo, D. Engineering and control of biological systems: A new way to tackle complex diseases. *FEBS Lett* **586**, 2122–2128 (2012).
9. Kitada, T., DiAndreth, B., Teague, B. & Weiss, R. Programming gene and engineered-cell therapies with synthetic biology. *Science* vol. 359 Preprint at https://doi.org/10.1126/science.aad1067 (2018).
10. Proteins, S. Chapter 13 Expressed Protein Modifi cations : Making. *Methods* **813**, 211–225 (2012).
11. Manhas, J., Edelstein, H. I., Leonard, J. N. & Morsut, L. The evolution of synthetic receptor systems. *Nat Chem Biol* **18**, 244–255 (2022).
12. Kwong, G. A. *et al.* Synthetic biomarkers: a twenty-first century path to early cancer detection. *Nature Reviews Cancer* vol. 21 655–668 Preprint at https://doi.org/10.1038/s41568-021-00389-3 (2021).

13. June, C. H., O'Connor, R. S., Kawalekar, O. U., Ghassemi, S. & Milone, M. C. CAR T cell immunotherapy for human cancer. *Science (1979)* **359**, 1361–1365 (2018).
14. Vishwasrao, P., Hui, S. K., Smith, D. L. & Khairnar, V. Role of NK Cells in Cancer and Immunotherapy. *Onco* **1**, 158–175 (2021).
15. Meng, Q. Y., Cong, H. L., Hu, H. & Xu, F. J. Rational design and latest advances of codelivery systems for cancer therapy. *Mater Today Bio* **7**, (2020).
16. Singh, V. K., Kalsan, M., Kumar, N., Saini, A. & Chandra, R. Induced pluripotent stem cells: Applications in regenerative medicine, disease modeling, and drug discovery. *Front Cell Dev Biol* **3**, 1–18 (2015).
17. Enterline, A. J. & Linebarger, C. Win, Lose, or Draw: Third Party Intervention and the Duration and Outcomes of Civil Wars. *What Do We Know about Civil Wars?* **480**, 93–108 (2016).
18. de Visser, K. E. & Joyce, J. A. The evolving tumor microenvironment: From cancer initiation to metastatic outgrowth. *Cancer Cell* **41**, 374–403 (2023).
19. Galon, J. No Title. **1960**, (2009).
20. Galon, J. & Bruni, D. Approaches to treat immune hot, altered and cold tumours with combination immunotherapies. *Nat Rev Drug Discov* **18**, 197–218 (2019).
21. Tormoen, G. W., Crittenden, M. R. & Gough, M. J. Role of the immunosuppressive microenvironment in immunotherapy. *Adv Radiat Oncol* **3**, 520–526 (2018).
22. Ouyang, P. *et al.* Overcoming cold tumors: a combination strategy of immune checkpoint inhibitors. *Front Immunol* **15**, 1–18 (2024).
23. Chen, D. S. & Mellman, I. Elements of cancer immunity and the cancer-immune set point. *Nature* **541**, 321–330 (2017).
24. Khosravi, G. R. *et al.* Immunologic tumor microenvironment modulators for turning cold tumors hot. *Cancer Commun* **44**, 521–553 (2024).

25. Fridman, W. H., Pagès, F., Sautès-Fridman, C. & Galon, J. The immune contexture in human tumours: Impact on clinical outcome. *Nat Rev Cancer* **12**, 298–306 (2012).
26. Duan, Q., Zhang, H., Zheng, J. & Zhang, L. Turning Cold into Hot: Firing up the Tumor Microenvironment. *Trends Cancer* **6**, 605–618 (2020).
27. Wang, L. *et al.* Hot and cold tumors: Immunological features and the therapeutic strategies. *MedComm (Beijing)* **4**, 1–21 (2023).
28. Benoit, A., Vogin, G., Duhem, C., Berchem, G. & Janji, B. Lighting Up the Fire in the Microenvironment of Cold Tumors: A Major Challenge to Improve Cancer Immunotherapy. *Cells* **12**, 1–21 (2023).
29. Mantovani, A., Marchesi, F., Malesci, A., Laghi, L. & Allavena, P. Tumour-associated macrophages as treatment targets in oncology. *Nat Rev Clin Oncol* **14**, 399–416 (2017).
30. Locati, M., Curtale, G. & Mantovani, A. Diversity, Mechanisms, and Significance of Macrophage Plasticity. *Annual Review of Pathology: Mechanisms of Disease* **15**, 123–147 (2020).
31. Ruffell, B. & Coussens, L. M. Macrophages and therapeutic resistance in cancer. *Cancer Cell* **27**, 462–472 (2015).
32. Yang, L. & Zhang, Y. Tumor-associated macrophages: from basic research to clinical application. *J Hematol Oncol* **10**, 58 (2017).
33. Cassetta, L. & Pollard, J. W. Targeting macrophages: Therapeutic approaches in cancer. *Nat Rev Drug Discov* **17**, 887–904 (2018).
34. Kloosterman, D. J. & Akkari, L. Macrophages at the interface of the co-evolving cancer ecosystem. *Cell* **186**, 1627–1651 (2023).
35. Curvello, R., Berndt, N., Hauser, S. & Loessner, D. Recreating metabolic interactions of the tumour microenvironment. *Trends in Endocrinology and Metabolism* **35**, 518–532 (2024).
36. Guo, Q. *et al.* Tumor microenvironment of cancer stem cells: Perspectives on cancer stem cell targeting. *Genes Dis* **11**, 101043 (2024).

37. Yang, Q. *et al.* The role of tumor-associated macrophages (TAMs) in tumor progression and relevant advance in targeted therapy. *Acta Pharm Sin B* **10**, 2156–2170 (2020).
38. Duan, Z. & Luo, Y. Targeting macrophages in cancer immunotherapy. *Signal Transduct Target Ther* **6**, 1–21 (2021).
39. Katkar, G. & Ghosh, P. Macrophage states: there's a method in the madness. *Trends Immunol* **44**, 954–964 (2023).
40. Orecchioni, M., Ghosheh, Y., Pramod, A. B. & Ley, K. Macrophage polarization: Different gene signatures in M1(Lps+) vs. Classically and M2(LPS-) vs. Alternatively activated macrophages. *Front Immunol* **10**, 1–14 (2019).
41. Chanmee, T., Ontong, P., Konno, K. & Itano, N. Tumor-associated macrophages as major players in the tumor microenvironment. *Cancers (Basel)* **6**, 1670–1690 (2014).
42. Wang, S. *et al.* Targeting M2-like tumor-associated macrophages is a potential therapeutic approach to overcome antitumor drug resistance. *NPJ Precis Oncol* **8**, (2024).
43. Chen, S. *et al.* Macrophages in immunoregulation and therapeutics. *Signal Transduct Target Ther* **8**, (2023).
44. Liu, J., Geng, X., Hou, J. & Wu, G. New insights into M1/M2 macrophages: key modulators in cancer progression. *Cancer Cell Int* **21**, 1–7 (2021).
45. Yunna, C., Mengru, H., Lei, W. & Weidong, C. Macrophage M1/M2 polarization. *Eur J Pharmacol* **877**, 173090 (2020).
46. Jayasingam, S. D. *et al.* Evaluating the Polarization of Tumor-Associated Macrophages Into M1 and M2 Phenotypes in Human Cancer Tissue: Technicalities and Challenges in Routine Clinical Practice. *Front Oncol* **9**, 1–9 (2020).
47. Georgoudaki, A. M. *et al.* Reprogramming Tumor-Associated Macrophages by Antibody Targeting Inhibits Cancer Progression and Metastasis. *Cell Rep* **15**, 2000–2011 (2016).
48. Pizzurro, G. A. & Miller-Jensen, K. Reframing macrophage diversity with network motifs. *Trends Immunol* **44**, 965–970 (2023).

49. Pan, Y., Yu, Y., Wang, X. & Zhang, T. Tumor-Associated Macrophages in Tumor Immunity. *Front Immunol* **11**, (2020).
50. Liu, M., Liu, L., Song, Y., Li, W. & Xu, L. Targeting macrophages: a novel treatment strategy in solid tumors. *J Transl Med* **20**, 1–28 (2022).
51. Lorestani, P. *et al.* The complex role of macrophages in pancreatic cancer tumor microenvironment: a review on cancer progression and potential therapeutic targets. *Discover Oncology* **15**, (2024).
52. Guan, W. *et al.* Tumor-associated macrophage promotes the survival of cancer cells upon docetaxel chemotherapy via the csf1/csf1r–cxcl12/cxcr4 axis in castration-resistant prostate cancer. *Genes (Basel)* **12**, (2021).
53. Demir, A. B. Tumor Promoting Inflammation. *Curr Mol Biol Rep* **9**, 21–32 (2023).
54. Yu, J. *et al.* Liver metastasis restrains immunotherapy efficacy via macrophage-mediated T cell elimination. *Nat Med* **27**, 152–164 (2021).
55. Bader, J. E. *et al.* PD-1 is induced on tumor-associated macrophages in obesity to directly restrain anti-tumor immunity. *bioRxiv* 2022.11.12.515348 (2022).
56. Peranzoni, E. *et al.* Macrophages impede CD8 T cells from reaching tumor cells and limit the efficacy of anti–PD-1 treatment. *Proc Natl Acad Sci U S A* **115**, E4041–E4050 (2018).
57. Kowal, J., Kornete, M. & Joyce, J. A. Re-education of macrophages as a therapeutic strategy in cancer. *Immunotherapy* **11**, 677–689 (2019).
58. Wangt, H. & Ullricht, A. 386181a0. **386113**, 181–186 (1997).
59. Veillette, A., Thibaudeaut, E. & Latour, S. High expression of inhibitory receptor SHPS-1 and its association with protein-tyrosine phosphatase SHP-1 in macrophages. *Journal of Biological Chemistry* **273**, 22719–22728 (1998).
60. Fujioka, Y. *et al.* A Novel Membrane Glycoprotein, SHPS-1, That Binds the SH2-Domain-Containing Protein Tyrosine Phosphatase SHP-2 in Response to Mitogens and Cell Adhesion. *Mol Cell Biol* **16**, 6887–6899 (1996).

61. Eladl, E. *et al.* Role of CD47 in Hematological Malignancies. *Journal of Hematology and Oncology* vol. 13 Preprint at https://doi.org/10.1186/s13045-020-00930-1 (2020).
62. MICHA, R. 乳鼠心肌提取 HHS Public Access. *Physiol Behav* **176**, 100–106 (2017).
63. Pietsch, E. C. *et al.* Anti-leukemic activity and tolerability of anti-human CD47 monoclonal antibodies. *Blood Cancer J* **7**, e536-8 (2017).
64. Tsai, R. K. & Discher, D. E. Inhibition of 'self' engulfment through deactivation of myosin-II at the phagocytic synapse between human cells. *Journal of Cell Biology* **180**, 989–1003 (2008).
65. Zhu, S., Wang, Y., Tang, J. & Cao, M. Radiotherapy induced immunogenic cell death by remodeling tumor immune microenvironment. *Front Immunol* **13**, 1–20 (2022).
66. Advani, R. *et al.* HHS Public Access. **379**, 1711–1721 (2021).
67. Jiang, C. *et al.* Targeting the CD47/SIRPα pathway in malignancies: recent progress, difficulties and future perspectives. *Front Oncol* **14**, (2024).
68. Barkal, A. A. *et al.* CD24 signalling through macrophage Siglec-10 is a target for cancer immunotherapy. *Nature* **572**, 392–396 (2019).
69. Sagiv, E. *et al.* Targeting CD24 for treatment of colorectal and pancreatic cancer by monoclonal antibodies or small interfering RNA. *Cancer Res* **68**, 2803–2812 (2008).
70. Kristiansen, G. *et al. CD24 Is Expressed in Ovarian Cancer and Is a New Independent Prognostic Marker of Patient Survival*.
71. Baumann, P. *et al.* CD24 expression causes the acquisition of multiple cellular properties associated with tumor growth and metastasis. *Cancer Res* **65**, 10783–10793 (2005).
72. Zarn, J. A., Zimmermann, S. M., Pass, M. K., Waibel, R. & Stahel, R. A. *Association of CD24 with the Kinase C-Fgr in a Small Cell Lung Cancer Cell Line and with the Kinase Lyn in an Erythroleukemia Cell Line*. *BIOCHEMICAL AND BIOPHYSICAL RESEARCH COMMUNICATIONS* vol. 225 (1996).

73. Li, W., Wang, F., Guo, R., Bian, Z. & Song, Y. Targeting macrophages in hematological malignancies: recent advances and future directions. *Journal of Hematology and Oncology* vol. 15 Preprint at https://doi.org/10.1186/s13045-022-01328-x (2022).
74. *A 1 2 3 4 5 6 7 8*.
75. Munday, J. *et al. Identification, Characterization and Leucocyte Expression of Siglec-10, a Novel Human Sialic Acid-Binding Receptor*. *Biochem. J* vol. 355 www.ebi.ac.uk (2001).
76. Zeller, T. *et al.* Perspectives of targeting LILRB1 in innate and adaptive immune checkpoint therapy of cancer. *Frontiers in Immunology* vol. 14 Preprint at https://doi.org/10.3389/fimmu.2023.1240275 (2023).
77. Barkal, A. A. *et al.* Engagement of MHC class i by the inhibitory receptor LILRB1 suppresses macrophages and is a target of cancer immunotherapy article. *Nat Immunol* **19**, 76–84 (2018).
78. Samaridis, J. & Colonna, M. *Cloning of Novel Immunoglobulin Superfamily Receptors Expressed on Human Myeloid and Lymphoid Cells: Structural Evidence for New Stimulatory and Inhibitory Pathways*. *Eur. J. Immunol* vol. 27 (1997).
79. Colonna, M. *et al. A Common Inhibitory Receptor for Major Histocompatibility Complex Class I Molecules on Human Lymphoid and Myelomonocytic Cells*. *J. Exp. Med* vol. 186 http://www.jem.org (1997).
80. Wang, Y. *et al.* Dendritic cell biology and its role in tumor immunotherapy. *Journal of Hematology and Oncology* vol. 13 Preprint at https://doi.org/10.1186/s13045-020-00939-6 (2020).
81. Chen, H. *et al.* Antagonistic anti-LILRB1 monoclonal antibody regulates antitumor functions of natural killer cells. *J Immunother Cancer* **8**, (2020).
82. Kuroki, K. *et al.* Structural and Functional Basis for LILRB Immune Checkpoint Receptor Recognition of HLA-G Isoforms. *The Journal of Immunology* **203**, 3386–3394 (2019).

83. Lu, C. H. *et al.* Involvement of M1 macrophage polarization in endosomal Toll-like receptors activated psoriatic inflammation. *Mediators Inflamm* **2018**, (2018).
84. McKiel, L. A., Woodhouse, K. A. & Fitzpatrick, L. E. The role of Toll-like receptor signaling in the macrophage response to implanted materials. *MRS Communications* vol. 10 55–68 Preprint at https://doi.org/10.1557/mrc.2019.154 (2020).
85. Kawasaki, T. & Kawai, T. Toll-like receptor signaling pathways. *Frontiers in Immunology* vol. 5 Preprint at https://doi.org/10.3389/fimmu.2014.00461 (2014).
86. Lee, J. *et al.* TLR5 agonist in combination with anti-PD-1 treatment enhances anti-tumor effect through M1/M2 macrophage polarization shift and CD8+ T cell priming. *Cancer Immunology, Immunotherapy* **73**, (2024).
87. Luo, M., Zhao, F., Cheng, H., Su, M. & Wang, Y. Macrophage polarization: an important role in inflammatory diseases. *Frontiers in Immunology* vol. 15 Preprint at https://doi.org/10.3389/fimmu.2024.1352946 (2024).
88. Zeng, Q. & Jewell, C. M. Directing toll-like receptor signaling in macrophages to enhance tumor immunotherapy. *Current Opinion in Biotechnology* vol. 60 138–145 Preprint at https://doi.org/10.1016/j.copbio.2019.01.010 (2019).
89. Xia, P. *et al.* Research progress on Toll-like receptor signal transduction and its roles in antimicrobial immune responses. doi:10.1007/s00253-021-11406-8/Published.
90. Grassin-Delyle, S. *et al.* The Role of Toll-Like Receptors in the Production of Cytokines by Human Lung Macrophages. *J Innate Immun* **12**, 63–73 (2020).
91. Underbill, D. M. & Gantner, B. Integration of Toll-like receptor and phagocytic signaling for tailored immunity. *Microbes and Infection* vol. 6 1368–1373 Preprint at https://doi.org/10.1016/j.micinf.2004.08.016 (2004).

92. Moyes, K. W. *et al.* Genetically Engineered Macrophages: A Potential Platform for Cancer Immunotherapy. *Hum Gene Ther* **28**, 200–215 (2017).
93. Mishra, A. K. *et al.* Macrophages as a Potential Immunotherapeutic Target in Solid Cancers. *Vaccines* vol. 11 Preprint at https://doi.org/10.3390/vaccines11010055 (2023).
94. Hadiloo, K., Taremi, S., Heidari, M. & Esmaeilzadeh, A. The CAR macrophage cells, a novel generation of chimeric antigen-based approach against solid tumors. *Biomarker Research* vol. 11 Preprint at https://doi.org/10.1186/s40364-023-00537-x (2023).
95. Sloas, C., Gill, S. & Klichinsky, M. Engineered CAR-Macrophages as Adoptive Immunotherapies for Solid Tumors. *Frontiers in Immunology* vol. 12 Preprint at https://doi.org/10.3389/fimmu.2021.783305 (2021).
96. Sterner, R. C. & Sterner, R. M. CAR-T cell therapy: current limitations and potential strategies. *Blood Cancer Journal* vol. 11 Preprint at https://doi.org/10.1038/s41408-021-00459-7 (2021).
97. Huang, T., Bei, C., Hu, Z. & Li, Y. CAR-macrophage: Breaking new ground in cellular immunotherapy. *Front Cell Dev Biol* **12**, 1464218 (2024).
98. Klichinsky, M. *et al.* Human chimeric antigen receptor macrophages for cancer immunotherapy. *Nat Biotechnol* **38**, 947–953 (2020).
99. Lei, A. *et al.* A second-generation M1-polarized CAR macrophage with antitumor efficacy. *Nat Immunol* **25**, 102–116 (2024).
100. Morsut, L. *et al.* Engineering Customized Cell Sensing and Response Behaviors Using Synthetic Notch Receptors. *Cell* **164**, 780–791 (2016).
101. Roybal, K. T. *et al.* Engineering T Cells with Customized Therapeutic Response Programs Using Synthetic Notch Receptors. *Cell* **167**, 419-432.e16 (2016).
102. Semeniuk, S., Qian, B.-Z. & Cachat, E. Engineering an anti-CD206-synNotch receptor: insights into the development of novel synthetic receptors. doi:10.1101/2024.02.07.579082.

103. Sloas, C., Gill, S. & Klichinsky, M. Engineered CAR-Macrophages as Adoptive Immunotherapies for Solid Tumors. *Frontiers in Immunology* vol. 12 Preprint at https://doi.org/10.3389/fimmu.2021.783305 (2021).
104. Wang, L., Chen, Y., Liu, X., Li, Z. & Dai, X. The Application of CRISPR/Cas9 Technology for Cancer Immunotherapy: Current Status and Problems. *Frontiers in Oncology* vol. 11 Preprint at https://doi.org/10.3389/fonc.2021.704999 (2022).
105. Zhang, H. *et al.* CRISPR/Cas9-mediated gene editing in human iPSCDerived macrophage reveals lysosomal acid lipase function in human macrophages-brief report. *Arterioscler Thromb Vasc Biol* **37**, 2156–2160 (2017).
106. Gong, Y. *et al.* Engineering nanoparticles-enabled tumor-associated macrophages repolarization and phagocytosis restoration for enhanced cancer immunotherapy. *J Nanobiotechnology* **22**, (2024).
107. Zhang, F. *et al.* Genetic programming of macrophages to perform anti-tumor functions using targeted mRNA nanocarriers. *Nat Commun* **10**, (2019).
108. Glass, E. B. *et al.* Stimulating TAM-mediated anti-tumor immunity with mannose-decorated nanoparticles in ovarian cancer. *BMC Cancer* **22**, (2022).
109. Chen, S. *et al.* Nanoparticles targeting tumor-associated macrophages: A novel anti-tumor therapy. *Nano Research* vol. 15 2177–2195 Preprint at https://doi.org/10.1007/s12274-021-3781-5 (2022).
110. Qu, T., Li, B. & Wang, Y. Targeting CD47/SIRPα as a therapeutic strategy, where we are and where we are headed. *Biomarker Research* vol. 10 Preprint at https://doi.org/10.1186/s40364-022-00373-5 (2022).
111. Maute, R., Xu, J. & Weissman, I. L. CD47–SIRPα-targeted therapeutics: status and prospects. *Immuno-Oncology and Technology* vol. 13 Preprint at https://doi.org/10.1016/j.iotech.2022.100070 (2022).
112. Liu, J. *et al.* Pre-clinical development of a humanized anti-CD47 antibody with anti-cancer therapeutic potential. *PLoS One* **10**, (2015).

113. Kauder, S. E. *et al.* ALX148 blocks CD47 and enhances innate and adaptive antitumor immunity with a favorable safety profile. *PLoS One* **13**, (2018).
114. Weiskopf, K. *et al.* Engineered SIRPα variants as immunotherapeutic adjuvants to anticancer antibodies. *Science (1979)* **341**, 88–91 (2013).
115. Billerhart, M. *et al.* CD47-targeted cancer immunogene therapy: Secreted SIRPα-Fc fusion protein eradicates tumors by macrophage and NK cell activation. *Mol Ther Oncolytics* **23**, 192–204 (2021).
116. Manuscript, S. Combination of NY-ESO-1-TCR-T-cells coengineered to secrete SiRP. 1–67 (2023).
117. [redacted]
118. Jin, C., Ma, J., Ramachandran, M., Yu, D. & Essand, M. CAR T cells expressing a bacterial virulence factor trigger potent bystander antitumour responses in solid cancers. *Nat Biomed Eng* **6**, 830–841 (2022).
119. Chen, Q., Guo, X. & Ma, W. Opportunities and challenges of CD47-targeted therapy in cancer immunotherapy. *Oncology Research* vol. 32 49–60 Preprint at https://doi.org/10.32604/or.2023.042383 (2024).
120. Chen, Y. C., Shi, W., Shi, J. J. & Lu, J. J. Progress of CD47 immune checkpoint blockade agents in anticancer therapy: a hematotoxic perspective. *Journal of Cancer Research and Clinical Oncology* vol. 148 Preprint at https://doi.org/10.1007/s00432-021-03815-z (2022).
121. Huang, Y., Ma, Y., Gao, P. & Yao, Z. Targeting CD47: The achievements and concerns of current studies on cancer immunotherapy. *J Thorac Dis* **9**, E168–E174 (2017).
122. Billerhart, M. *et al.* CD47-targeted cancer immunogene therapy: Secreted SIRPα-Fc fusion protein eradicates tumors by macrophage and NK cell activation. *Mol Ther Oncolytics* **23**, 192–204 (2021).
123. Fonseca, J. P., Bonny, A. R., Town, J. & El-Samad, H. Assembly of Genetic Circuits with the Mammalian ToolKit. *Bio Protoc* **10**, (2020).

124. Zhu, I. *et al.* Modular design of synthetic receptors for programmed gene regulation in cell therapies. *Cell* **185**, 1431-1443.e16 (2022).
125. Heideveld, E. *et al. Methods for Macrophage Differentiation and in Vitro Generation of Human Tumor Associated-like Macrophages*. *Methods in Enzymology* vol. 632 (Elsevier Inc., 2020).
126. Baxter, E. W. *et al.* Standardized protocols for differentiation of THP-1 cells to macrophages with distinct M(IFNγ+LPS), M(IL-4) and M(IL-10) phenotypes. *J Immunol Methods* **478**, (2020).
127. Benner, B. *et al.* Generation of monocyte-derived tumor-associated macrophages using tumor-conditioned media provides a novel method to study tumor-associated macrophages in vitro. *J Immunother Cancer* **7**, 1–14 (2019).
128. Zhang, Y., Zhang, Z., Chen, L. & Zhang, X. Tumor cells-derived conditioned medium induced pro-tumoral phenotypes in macrophages through calcium-nuclear factor κB interaction. *BMC Cancer* **22**, 1–18 (2022).
129. Liu, R. *et al.* CD47 promotes ovarian cancer progression by inhibiting macrophage phagocytosis. *Oncotarget* **8**, 39021–39032 (2017).